

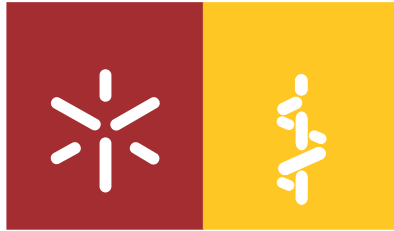


Universidade do Minho
Escola de Ciências da Saúde

Ana Raquel Abrunhosa Carvalho de Lima

Neuron-astrocyte interactions in complex cognitive functions

Interações neurónio-astrocítico em funções cognitivas complexas



Universidade do Minho

Escola de Ciências da Saúde

Ana Raquel Abrunhosa Carvalho de Lima

**Neuron-astrocyte interactions in complex
cognitive functions**

**Interacções neurónio-astrócito em
funções cognitivas complexas**

Dissertação de Mestrado
Mestrado em Ciências da Saúde

Trabalho realizado sob a orientação do
Doutor João Oliveira

DECLARAÇÃO

Nome: Ana Raquel Abrunhosa Carvalho de Lima

Endereço Electrónico: analima@ecsaude.uminho.pt

Telefone: 919926722

Nº de Bilhete de Identidade: 13459797

Título da dissertação: NEURON-ASTROCYTE INTERACTIONS IN COMPLEX COGNITIVE FUNCTIONS

Orientador: Doutor João Oliveira

Ano de conclusão: 2012

Ramo de Conhecimento do Mestrado:

Ciências da Saúde - Ciências da Saúde

É AUTORIZADA A REPRODUÇÃO INTEGRAL DESTA TESE/TRABALHO APENAS PARA EFEITOS DE INVESTIGAÇÃO, MEDIANTE DECLARAÇÃO ESCRITA DO INTERESSADO QUE A TAL SE COMPROMETE.

Universidade do Minho, 3 de Setembro de 2012

Assinatura: _____

AGRADECIMENTOS

Em primeiro lugar quero agradecer à minha família. Aos meus pais que me apoiaram não só na decisão de ingressar neste mestrado, como também em todos os momentos mais desafiantes. Ao meu irmão caçula, André, por ser o Peixe-Beijoca, perito em gargalhadas que me animaram durante este ano. Ao meu irmão Pedro por partilhar comigo a filosofia do pumba-arrebentismo que me desvia do stresse e me devolve alguma sanidade mental. À minha tia Olga e à minha prima Inês (ou simplesmente a Prima), pelos momentos de descontração proporcionados nos fins de semana. Aos meus avós por me terem acolhido tão bem deste lado e pela oportunidade que me proporcionaram.

Agradeço ao Leonel por todo o apoio nas maratonas de trabalho, pela paciência para aturar pseudo-estados depressivos, por me dar ânimo quando eu achava que já não conseguia mais, por me deixar fazer dos seus caracóis bola anti-stresse, por me acompanhar nas maratonas culinárias quando me apetecia jantar algo de diferente e estupidamente calórico... e por todo o carinho, é claro.

À Sofi e à Vi, agradeço pelo constante apoio, mesmo estando distantes no meio dos seus PhDs. Ao Sérgio e ao Hugo por darem apoio psicológico ao Leonel depois de me aturar...espero que tenha resultado!

Quero também agradecer ao João Oliveira, por ter acreditado em mim para iniciar este projecto de raiz, numa área na qual me vim a viciar, e pelos “dá-lhe giz” que me fizeram lutar ainda mais pelos objectivos.

Aos NeRDs, agradeço pela boa disposição geral e também pelo *input* científico. À Fernanda Marques, pela ajuda com os PCRs e à Luísa Pinto pelas dicas com as imunos. À Su e ao Sandro e Mónica, pelas conversas de corredor e de bar que me recarregavam as energias instantaneamente. À Su novamente por me ajudar com mil e uma cenas, à Mónica também por me ajudar com as imunos que teimavam em não funcionar. À Sofia e à Cristina, por ajudarem também a apagar alguns “fogos”. Às meninas do melhor *open space*: à Silvina pelas dicas zen; à Filipa pela constante alegria *no matter what*; à Magdinha pré- e pós-astrocítica por me acompanhar e ajudar nesta aventura; à Vanessa pela ajuda nesta fase final e pela energia que só uma Sardinha poderia ter!

Muito obrigada a todos!

ABSTRACT

Since the arousal of the “glia” concept, 150 years ago, the knowledge on the features of glial cells, especially astrocytes, has been dramatically evolving. These star-shaped cells that lack axons not only participate in brain metabolism, supporting neuronal activity, but also can modulate the neurotransmission by modulating synapses. From taking part in the “tripartite synapse” to the astrocytic excitability - based on intracellular Ca^{2+} increases - and gliotransmission, astrocytes have been given the relevance that raises the idea that such glial modulation at cellular level should have greater implications in higher brain functions. However, these remarkable astrocytic features, as well as its influence in modulation of behaviour outputs, are still under-explored. In the attempt to contribute to the progress of our knowledge on these cells purpose in the brain, we decided to investigate the astrocytic component of the neuron-astrocyte interactions in complex cognitive processes that rely on the prefrontal cortex, analysing the behavioural performance of two animal models of astrocytic pathology. For that purpose, we implemented a rat model of pharmacological astrocytic ablation in the medial prefrontal cortex, through bilateral intracranial injections of the gliotoxin L- α -aminoadipate, and the transgenic dnSNARE mouse model, that displays conditional blockade of gliotransmitters vesicular release in astrocytes.

From the behaviour assessment of the rats subjected to the bilateral intracranial injections of L- α -aminoadipate we could conclude that the astrocytic ablation in the medial prefrontal cortex affects the attentional set-shifting, the working memory and the reversal learning. Microscope analysis of brain sections of the gliotoxin-injected animals revealed that astrocyte depleted regions were confined to the prelimbic and cingulate cortex, where the neuronal population was not affected. The genetic mouse model of conditional blockade of vesicular release in astrocytes was characterised in a more extensive way. We show here that these animals do not display anxious phenotype or have locomotor difficulties. Most importantly dnSNARE animals have shown impaired spatial reference memory (hippocampus-dependent) and improved working memory, but normal reversal learning (prefrontal cortex-dependent functions). Both astrocytes and gliotransmission seem to be crucial for cognitive computation and may represent a new window of understanding of brain function that urges to be clarified in terms of cellular pathways and biochemical mechanisms.

The successful implementation of both animal models of differential astrocytic pathology, at the ICVS will allow further studies in our lab. Despite our interesting results additional studies are required to help the elucidation of the mechanisms involved, such as using electrophysiological and neurochemical techniques to understand how brain dynamic is altered, either in healthy or in pathological states.

RESUMO

Desde há 150 anos, quando surgiu o conceito de “glia”, que o conhecimento das funções das células da glia, especialmente dos astrócitos, tem vindo a evoluir drasticamente. Estas células em forma de estrela e sem axónios, não só participam no metabolismo de cérebro como também contribuem para uma boa actividade neuronal, modelando até a actividade sináptica e o fluxo de neurotransmissores. Por fazerem parte da “sinapse tripartida”, exibirem uma forma de excitabilidade - baseada em elevações de Ca^{2+} intracelulares - e realizarem gliotransmissão, os astrócitos têm recebido a relevância que levanta a questão de que tais células poderão ter maiores implicações nas funções cerebrais. Contudo, estas características notáveis bem como a sua influência na modulação do comportamento não estão ainda clarificadas. Por isso, na tentativa de contribuir para o progresso do nosso conhecimento acerca da função destas células no cérebro, decidimos investigar a componente astrocítica nas interacções neurónio-astrócito no contexto das funções cognitivas complexas dependentes do córtex pré-frontal, analisando a performance comportamental de dois modelos animais de patologia astrocítica: um modelo de rato na qual provocámos a ablação de astrócitos no córtex pré-frontal medial, através de injeções bilaterais intracranianas da gliotoxina L- α -aminoadipato; e um modelo genético em ratinho, dnSNARE, que exhibe um bloqueio condicional da libertação vesicular de gliotransmissores nos astrócitos.

Da análise comportamental do modelo de rato, concluímos que a ablação de astrócitos no córtex pré-frontal medial afecta o *attentional set-shifting*, a memória de trabalho e a aprendizagem reversa. A análise microscópica de secções de cérebro dos ratos injectados com a gliotoxina revelou que as regiões de ablação astrocítica estavam confinadas ao córtex pré-límbico e córtex cingulado, onde a população neuronal não estava afectada. Uma caracterização mais extensiva do modelo de ratinhos dnSNARE revelou que estes animais não exibem fenótipo ansioso nem défices de locomoção, mas demonstram défices na memória de referência espacial (dependente do hipocampo), memória de trabalho melhorada e aprendizagem reversa normal (funções dependentes do córtex pré-frontal). Tanto os astrócitos como apenas a gliotransmissão aparentam ser cruciais para a computação cognitiva e representam uma nova janela de conhecimento que urge ser clarificada em termos de vias celulares e mecanismos bioquímicos.

Apesar dos resultados interessantes já obtidos com a implementação já bem sucedida destes modelos animais no ICVS, são necessários estudos mais aprofundados para ajudar na elucidação dos mecanismos envolvidos. Acreditamos que o recurso a técnicas de electrofisiologia e neuroquímica permitirá uma melhor compreensão de como o cérebro está alterado, quer em condição de saúde ou doença.

TABLE OF CONTENTS

AGRADECIMENTOS	iii
ABSTRACT	v
RESUMO	vii
INDEX OF FIGURES AND TABLES	xiii
LIST OF ABBREVIATIONS	xv
<hr/>	
1. INTRODUCTION	1
1.1. Astrocytes in the brain	1
1.1.1. Arousal and evolution of the astrocytic concept	1
1.1.2. Astroglia in brain metabolism	2
1.1.3. Modulation of the synaptic transmission: the tripartite synapse	3
1.1.4. Integration of neuron-glia circuits: from gap junctions to gliotransmission	4
1.2. Astrocytes in brain disorders	7
1.3. Astrocytic function in vivo: behaviour and cognition	8
1.4. The prefrontal cortex	8
1.4.1. Cognitive functions of the the prefrontal cortex: learning and memory	9
<hr/>	
2. AIM OF WORK	11
<hr/>	
3. MATERIALS AND METHODS	13
3.1. Animals and Treatments	13

3.1.1. Aminoadipate rat model of astrocytic depletion	13
3.1.1.A.Surgical procedure for the establishment of the pharmacological rat model	13
3.1.1.B.Drug preparation and administration	14
3.1.2. Transgenic dominant-negative SNARE mice (dnSNARE) genetic model	14
3.1.2.A.Colony management and genotyping	16
3.2. Behaviour Tests	17
3.2.1. Aminoadipate rat model of astrocytic depletion	17
3.2.1.A.Attentional set-shifting task	17
3.2.1.B.Water maze tests	21
3.2.2. dnSNARE mice model of impaired vesicular release in astrocytes	23
3.2.2.A.Elevated Plus Maze (EPM)	23
3.2.2.B.Open field test (OF)	24
3.2.2.C.Water maze tests	24
3.2.2.D.Continuous spontaneous alternation test	26
3.3. Histological procedures	27
3.3.1. Euthanasia and tissue preparation	27
3.3.2. Immunofluorescent staining of astrocytes and neurons	27
3.3.3. Microscopic analysis	28
3.3.3.A.Identification of lesion sites	28
3.3.3.B.Stereological analysis of the affected region	28
3.3.4. Statistical Analysis	29
<hr/>	
4. RESULTS	31

4.1. Aminoadipate pharmacological rat model	31
4.1.1. Selection of animals and lesion features	31
4.1.2. Behaviour performance	32
4.1.2.A.Attentional set-shifting task	32
4.1.2.B.Water maze based tests	35
4.2. dnSNARE mice model of impaired vesicular release in astrocytes	36
4.2.1. Genotyping and selection of animals	36
4.2.2. Behaviour performance	37
4.2.2.A.Elevated plus maze (EPM)	37
4.2.2.B.Open Field test (OF)	40
4.2.2.C.Water maze based tests	42
4.2.2.D.Continuous spontaneous alternation test	44
<hr/>	
5. DISCUSSION AND CONCLUSION	47
<hr/>	
6. REFERENCES	53

INDEX OF FIGURES AND TABLES

Figures

Figure 1.1	Astrocytes endfeet	2
Figure 1.2	The tripartite synapse	3
Figure 1.3	Modulation pathways of the synaptic transmission mediated by gap junctions.	4
Figure 1.4	Calcium-dependent vesicular release of gliotransmitters from astrocytes.	6
Figure 1.5	Highlights of the PFC and mPFC, in human brain evidencing the homology of mPFC and dlPFC brain regions in rat and human, respectively	9
Figure 3.1	Schematic representation of GFAP promotor driving the expression of the target gene dnSNARE and reporter gene EGFP in astrocytes.	15
Figure 3.2	Representation of the ASST apparatus.	18
Figure 3.3	Representation of the water maze tests apparatus, prepared for rats	22
Figure 3.4	Representation of the water maze tests apparatus, prepared for mice	25
Figure 3.5	Representation of the Y maze apparatus.	26
Figure 4.1	Representation of the sites of brain injection sites, 4.20 mm to 2.76 mm from Bregma	31
Figure 4.2	Effects of the gliotoxin L- α -AA.	33
Figure 4.3	Trials to criterion along ASST stages.	34
Figure 4.4	Indexes of Learning and Reversal.	34
Figure 4.5	Escape latencies (s) in water maze tests.	35
Figure 4.6	Performance of the rats in the reversal learning task, RLT and probe task of the water maze tests.	36
Figure 4.7.	Mice genotyping.	37
Figure 4.8.	Time spent (as percentage of total) in the arms and hub of the EPM.	38
Figure 4.9.	Number of entrances in open arms and closed arms of the EPM.	39
Figure 4.10	Number of explorations in open arms and closed arms of the EPM.	39
Figure 4.11	Distance travelled (cm) in the open field arena.	40
Figure 4.12	Velocity (cm/s) in the open field arena.	41
Figure 4.13	Number of rearings in the open field arena.	41

Figure 4.14	Time (as percentage of total) spent in the center of the open field arena.	42
Figure 4.15	Escape latency (s) in the spatial reference memory task, RMT.	43
Figure 4.16	Performance in the reversal learning task, RLT.	44
Figure 4.17	Arm alternation (alternation score, %) in the continuous spontaneous alternation task, performed in the Y-maze	45
Figure 4.18.	Total arm entries in the continuous spontaneous alternation task, performed in the Y-maze.	45

Tables

Table 3.1	PCR conditions used for the amplification of tTA and tet.O sequences.	17
Table 3.2	Order of discrimination stages, relevant and irrelevant dimensions, and stimuli combinations of ASST presented to the animals.	19
Table 3.3	Stimuli combinations and sequence of presentation along 10 trials of the simple discrimination, stages on test day one.	20
Table 3.4	Stimuli combinations and sequence of presentation along 10 trials of the test first compound discrimination and its reversal stages.	20
Table 3.5	Stimuli combinations and sequence of presentation along 10 trials of the test second compound discrimination and its reversal stages.	21
Table 3.6 .	Timeline followed in the water maze tests used for rat models of astrocytic ablation.	23
Table 3.7	Timeline followed in the water maze tests used for the mice models of astrocytic dysfunction.	26

LIST OF ABBREVIATIONS

♀	Female mice
♂	Male mice
AA	Group of animals injected with L- α -aminoadipate, in the pharmacological rat model
Aβ	amyloid- β
aCSF	Artificial Cerebrospinal Fluid
AMPA	α -amino-3-hydroxy-5-methyl-4-isoxazolepropionic acid
ASST	Attentional Set-Shifting Task
ATP	Adenosine 5'-triphosphate
Ca²⁺	Calcium ion
CDO	Compound discrimination of odours
Cg	Cingulate cortex
CON	Group of animals injected with aCSF, in the pharmacological rat model
dnSNARE	dominant-negative N-ethylmaleimide-sensitive factor attachment protein receptor
EDST	Extradimensional shifting for textures
EGFP	Enhanced Green Fluorescent Protein
EPM	Elevated Plus Maze
FBS	Fetal Bovine Serum
GABA	γ -amino-butyric acid
GFAP	Glial Fibrillary Acidic Protein
GLUT1	Glucose transporter 1
Gt	Gliotransmitters
H⁺	Hydrogen ion
i.p.	intraperitoneal
IL	Infralimbic cortex
IP3	Inositol (1, 4, 5)-triphosphate
IVCS	Life Sciences Research Institute
K⁺	Potassium ion
L-α-AA	L- α -Aminoadipate
mGluR	metabotropic glutamate receptors

mPFC	medial prefrontal cortex
NCX	Sodium/Calcium exchanger
NMDA	N-Methyl-D-aspartic acid
Nt	Neurotransmitters
OF	Open Field
PBS	Phosphate Buffer Saline
PCR	Polymerase Chain Reaction
PFC	Prefrontal Cortex
PrL	Prelimbic cortex
Q1	water maze imaginary quadrant 1
Q2	water maze imaginary quadrant 2
Q3	water maze imaginary quadrant 3
Q4	water maze imaginary quadrant 4
Rev1	Reversal of the compound discrimination stage
Rev2	Reference Memory Task
RLT	Reversal Learning Task
RMT	Reference Memory Task
SDO	Simple discrimination of odours
SDT	Simple discrimination of textures
SOCE	Store-operated Ca ²⁺ entry
TAE	Tris-Acetate-EDTA
TC	Trials to criterion
tetO	tet Operator
TNFα	Tumor necrosis factor α
tTA	Tetracycline-controlled transactivator protein
VAMP 2	Vesicle-associated membrane protein 2
VAMP 3	Vesicle-associated membrane protein 3
VGCC	Voltage-gated Ca ²⁺ channels
WMT	Working Memory Task

1. INTRODUCTION

1.1. *Astrocytes in the brain*

1.1.1. *Arousal and evolution of the astrocytic concept*

More than 150 years have passed since Rudolf Virchow shared his primordial ideas on the brain connective tissue, the “nervenkitt” or nerve-cement which he named “neuroglia” [1]. By neuroglia, that he would not believe to contain cellular elements, Rudolf Virchow referred to the supportive tissue “which lies between the proper nervous parts, hold them together and gives the whole its form in a greater or less degree” [2]. Camillo Golgi did not linger to establish the cellular nature of neuroglia [3, 4] and incredibly, this division between nerve elements and supportive tissue still persists to a large degree in the convictions of many neuroscientists [5]. Later in 1893, Michael von Lenhossek proposed the term “astrocyte”, further categorised in fibrous or protoplasmatic, located in white and grey matter, respectively [6, 7]. These studies were followed by Santiago Ramón y Cajal who further characterised astrocytes in brain tissue and anticipated that these cells should interact closely with neurons [8]. In addition to astrocytes oligodendrocytes and microglia, the other non-neural cells, were also included into the neuroglia concept by Pio del Rio-Hortega [9-11].

The concept of neuroglia (also termed glia) is now more than 150 years-old. However, our knowledge on the diversity and features of glial cells, especially astrocytes, has been dramatically changing. Despite many years of research that led to the arousal of new concepts attributing new roles to glial cells in brain function, their whole range of actions in the nervous system is still far from understood [5]. The first attributed role to glial cells, presented by the filing concept [2, 12] had a simple connotation because neuroglia was given a passive role as an element that fills “space not occupied by neurons”. Concerning the Virchow’s idea that the neuroglia holds nervous elements “together and gives the whole its form”, it was already proven that the architecture of the grey matter is defined by the astrocytes: protoplasmatic astrocytes occupy a certain territory and canton grey matter covering all neuronal elements within that domain [13, 14]. Moreover, astrocytes have been considered a homogenous cell population with a distinctive star-shaped morphology due to the numerous processes that extend to neurons and blood vessels, and that contain intermediate filaments (glial fibrils) [15].

Despite the fact that astrocytes lack axons and are not capable of generating actions potentials, several crucial functions have been attributed to these glial cells, including the

maintenance of the neuronal activity through extracellular homeostasis of potassium (K^+) and hydrogen (H^+) ions [16], maturation, survival during development and nutrient supply for neurons, release of growth factors, neurotransmitters uptake from the synaptic cleft, among others. Even though these functions are well-accepted, neuroscientists still believed that there was much more to be clarified [15].

1.1.2. Astroglia in brain metabolism

Golgi suggested that the purpose of astrocytes was to provide an environment suitable for neuronal function. The complex ultrastructure of astrocytes, makes them capable of being actively involved in neurotransmitter homeostasis [14, 17-20]. As a matter of fact, it is already recognised that astrocytes take up glutamate from the synaptic cleft and metabolise it into glutamine, via glutamine synthetase [21, 22], that is then given back to neurons for *de novo* synthesis of glutamate.

Besides buffering glutamate, astrocytes are also able to bridge the nutrient passage from blood to neurons - fig. 1.1. In fact, astrocytes present specialised processes, named endfeet, that project to the brain vasculature ensheathing the blood vessel walls [23, 24]. This astrocytic endfeet location at the capillaries combined with the abundant expression of the glucose transporter GLUT1 [25], create the perfect conditions for astrocytes to access glucose supply from blood. However, the flow of energetic substrates is not that straight forward. Another two substrates, glycogen and lactate are involved in the astrocytic regulation of neuronal metabolic activity. The synthesis of glycogen may occur as an alternative of glucose-6-phosphate metabolism, as a part of the glycogen-shunt [26, 27]. Apparently, there is an interdependence of glycogen-shunt activity and glycolysis that plays an important role in the supply of energy for the maintenance of glutamatergic activity [26, 28]. As reviewed by Brown and Ransom [29], upon increasing brain activation, when the immediate supply of neuronal glucose is depleted, glycogen metabolism can provide a rapid energy source that rate-limited the step of glucose phosphorylation via hexokinase. Equally

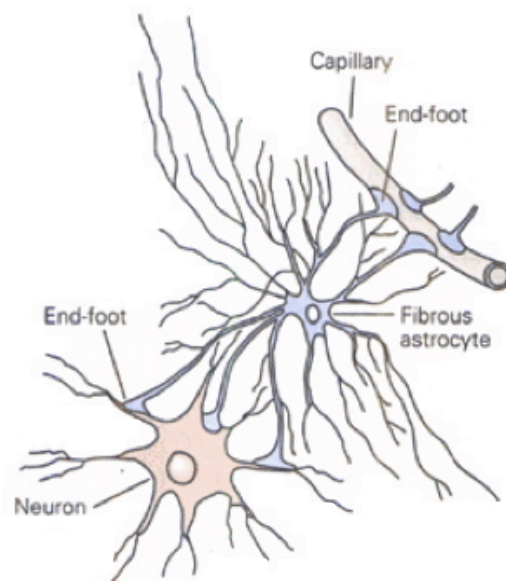


Figure 1.1. Astrocytes endfeet connecting brain capillaries to neurons to bridge the nutrient passage from blood [23].

important is the lactate as an oxidative substrate for energy metabolism, once it is generated in astrocytes during glutamate-glutamine cycle as consequence glutamate amidation [30, 31]. Because of these findings, a model coupling neuronal activation and glucose utilisation was proposed: the astrocyte-neuron lactate shuffle hypothesis [31]. Although research on brain metabolic pathways has been controversial, it is important to recognise that upon different conditions neurons may rely on glucose, glycogen or lactate to support brain function, as these energetic pathways are not mutually exclusive [15].

1.1.3. Modulation of the synaptic transmission: the tripartite synapse

The emerging of astrocyte-neuron interaction biology has been changing our perspective on the physiology of the nervous system. In fact, the classically accepted paradigm that brain function results exclusively from the neuronal activity is being challenged by recent findings, which rather strongly suggest that brain function arises from the concerted activity and crosstalk between neurons and astrocytes. In that context, the concept of “tripartite synapse” was proposed to conceptualise the occurrence of bidirectional communication between neurons and astrocytes [32]: neurotransmitters released from the presynaptic terminals of neurons can activate not only receptors on postsynaptic elements, but also on neighbouring

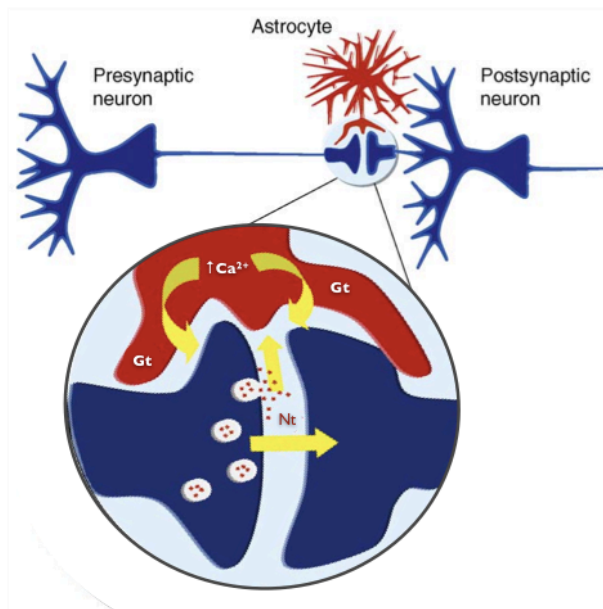


Figure 1.2. The tripartite synapse. Neurotransmitters (Nt) released in the synaptic cleft activate surrounding astrocytes that respond with Ca²⁺ elevations, leading to the modulation of the synaptic activity through the release of gliotransmitters (Gt). Adapted from Perea et al [34].

astrocytes which in turn signal back to neurons modulating the synaptic transmission [33, 34] - fig 1.2. More precisely, the cellular mechanisms that underlie the tripartite synapse concept are: (1) Neurotransmitters, such as glutamate, released from the presynaptic terminals of neurons can activate receptors on neighbouring astrocytes through the partial bounding to the metabotropic glutamate receptors (mGluR); (2) this activation leads to the production of inositol (1, 4, 5)-triphosphate (IP3) and release on calcium ions (Ca²⁺) from the endoplasmic reticulum to the cytoplasm of astrocytes; (3) these increases in intracellular Ca²⁺ concentration- a form of astrocytic excitability- are transmitted to

neighbour astrocytes as intercellular calcium waves, through gap junctions between astrocytes, and ATP, as diffusible messenger of Ca^{2+} to non-contiguous astrocytes [35, 36]; (4) the astrocytic excitability results in the release of gliotransmitters, including glutamate and ATP to the extracellular space; (5) the gliotransmitter release feeds back onto pre- and postsynaptic terminals culminating in the modulation of the synaptic activity. [37-41]. This model of tripartite synapse emphasises the fact that astrocytes are able to sense neuronal activity, considering that intra- and intercellular waves of Ca^{2+} are generated by neuronal signals [40, 42].

1.1.4. Integration of neuron-glia circuits: from gap junctions to gliotransmission

Gap junctions are key components on this remarkable feature of astrocytic excitability, and are thought to play a crucial role in the integration of neuronal-glia circuits. Indeed, most gap junctions in the brain occur in glial cells, and in particular in astrocytes, with a very high coupling strength. That astroglial coupling intensity confers a functional astrocytic syncytium, that not only forms a metabolic network that can provide energy supply to active neurons, but also implies high coordination in astroglial responses so synaptic events [41] - fig 1.3.

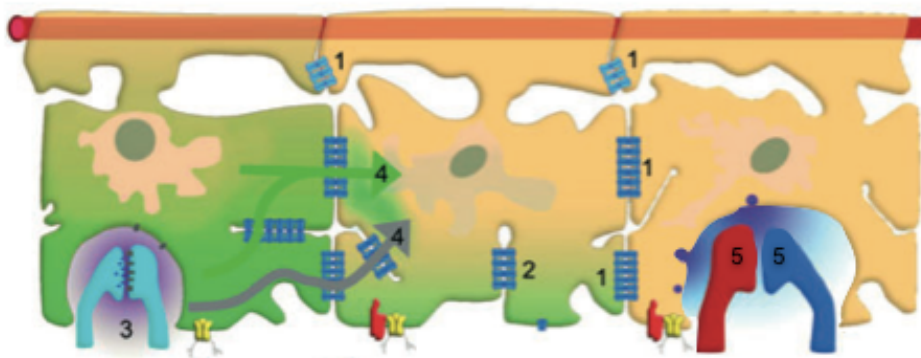


Figure 1.3. Modulation pathways of the synaptic transmission mediated by gap junctions. Either between astrocytes (1) or processes of the same cell (2), gap junctions facilitate the passage of ions, second messengers and nutrients. Synaptic activity (3) causes the production of IP3 (4, grey) and the release of Ca^{2+} (4, green) and the astrocytic excitability is transmitted through gap junctions to the neighbor astrocytes as calcium wave. Gliotransmission occurs as soon as the calcium wave is spread to the closest astrocyte in contact with a synapse, and culminates in the modulation of the synaptic activity (5). Adapted from Parpura *et al* [41].

Intercellular Ca^{2+} waves are a form of astrocyte signalling that not only occurs in response to neuronal activity, but may also appear spontaneously. Even so, they are believed to

provide a modulation pathway between domains of separate neurons [41]. That is because a single astrocyte can contact over one hundred thousand synapses, yet in a way that individual astrocytes occupy distinct and non-overlapping domains in the brain [13, 43]. Here arises the evidence that astrocytes respond to neuronal domains defined by them and not to individual neurons.

The bidirectional communication between neurons and astrocytes frequently involves modulation of synaptic transmission (by tripartite synapse) and plasticity (through dynamic GFAP expression upon different physiological conditions, such as synaptic receptor activation [44], and secondary messengers, like Ca^{2+} [45]) [32, 37, 46, 47]. The process by which astrocytes communicate with surrounding cells by the release of transmitters is called gliotransmission [48]. Those heterocellular signalling events in astrocytes often imply regulated exocytosis [49, 50], a process that requires vesicles containing a chemical transmitter or a blend of them. The secretion of gliotransmitters to the extracellular space occurs by the fusion of the vesicular and plasma membranes, upon a membrane merger. Once exocytosed, gliotransmitters can exert paracrine function, on adjacent cells, or autocrine function, on the cell which secreted them [51]. Moreover, gliotransmitters have been reported to act pre- and/or postsynaptically, modulating the synaptic transmission in a transient or long-lasting manner [41]. What determines the regulation of exocytosis is the increase of cytosolic [Ca^{2+}] that, in the case of astrocytes appears to be slower than in neurons [51]. Exocytotic vesicles released from astrocytes were described to contain diverse chemical transmitters, such as glutamate, D-serine, ATP, adenosine, GABA, tumor necrosis factor α ($\text{TNF}\alpha$), prostaglandins, proteins and peptides that can influence neuronal and synaptic physiology [52], blood flow, the permeability of the blood brain barrier and also provide metabolic support [5, 15, 34]. Glutamate is synthesised *de novo* in astrocytes as a by-product of Krebs cycle [21, 53]; D-serine is generated through the stereoisomeric conversion from L-serine by racemase, an enzyme found in astrocytes [54-56] ; ATP production results from aerobic respiration and, as stated above, can mediate intercellular signalling through purinergic receptors; but it is more frequent the hydrolysis of ATP by membrane-bound ectonucleotidases to adenosine-diphosphate so that adenosine can act on diverse plasma membrane receptors [57].

The synaptic transmission causes also the activation of strategically positioned ion flux pathways in astroglial perisynaptic processes. Upon activation through the release of ATP and/or glutamate, the ionotropic (P2X) and metabotropic receptors (α -amino-3-hydroxy-5-methyl-4-isoxazolepropionic acid, AMPA, and N-Methyl-D-aspartic acid, NMDA, receptors), glutamate transporters and sodium/calcium exchanger (NCX) [58-62] act in a concerted manner resulting in the modulation of the synaptic transmission and plasticity by affecting the time kinetics of glutamate removal from the synaptic cleft [41].

The sources of Ca^{2+} necessary for gliotransmission in astrocytes are diverse and complex. As a matter of fact there are multiple molecular entities acting to provide Ca^{2+} to drive Ca^{2+} - dependent regulated exocytosis. Calcium ions can be delivered from: (1) the ER lumen to the cytosol through IP₃- and ryanodine-sensitive receptors that serve as channels [63]; (2) through plasmallemal channels, across the astrocytic plasma membrane - in a process named store-operated Ca^{2+} entry (SOCE) [64, 65]-, ligand- and voltage-gated Ca^{2+} channels (VGCC) [66], and NCXs [67, 68] at the plasma membrane that mediate Ca^{2+} entry from the extracellular space to the cytosol, when ER Ca^{2+} is depleted; (3) mitochondrial matrix, as free Ca^{2+} exits through the mitochondrial NCX and transient openings of the mitochondrial permeability transition pore to the cytosol [69].

Recent findings demonstrated that gliotransmission can be modulated downstream to Ca^{2+} waves generation, most likely at the secretory machinery level, as observed in the case of glutamatergic output from astrocytes [70]. In fact, astrocytes express exocytotic secretory machinery proteins, specially the N-ethylmaleimide-sensitive factor attachment protein receptor (SNARE) complex, composed of: synaptobrevin 2- also called vesicle-associated membrane protein 2 (VAMP 2)- and its homologue cellubrevin - also called vesicle-associated membrane protein 3 (VAMP 3); syntaxins 1, 2 and 4; and synaptosome-associated protein of 23kDa (SNAP-23) [71, 72] - fig. 1.4.

Altogether, these astrocytic features allow direct or indirect interference with neural communication. Many reports (see section 1.1.3) have shown that astrocytes are able to modulate synaptic function, leading to and interference of the information processing at the network level, and consecutively in the network-output generation. Therefore it is highly predictable that astrocytes play a role in construction of behaviour outputs of a specific brain region. This aspect is relevant both in health and pathological states.

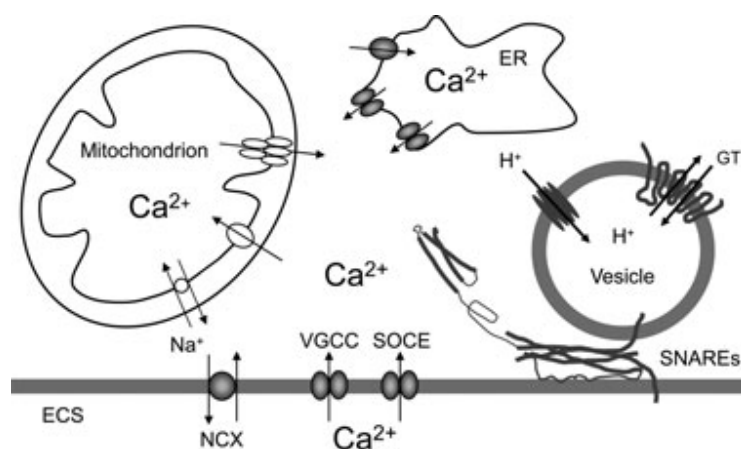


Figure 1.4. Calcium-dependent vesicular release of gliotransmitters from astrocytes: sources of Ca^{2+} and the formation of the SNARE complex necessary for gliotransmission in astrocytes [41].

1.2. *Astrocytes in brain disorders*

Astrocytic structure and protein expression were already shown to be altered in the context of brain disorders like depression, Parkinson's disease, Alzheimer's disease, epilepsy and schizophrenia [73-86]. What remains to understand is if astrocytic dysfunction constitutes the cause, providing detrimental signals that contribute to the disorder, or the consequence, performing a supportive function in the attempt to reverse and prevent the disorder. Hence it is important to investigate the contribution of astrocytes to network function in order to understand their role in pathophysiological states. Since gliotransmission is now known as a modulatory factor of synaptic communication (see section 1.1.3) it may be considered an important mechanism underlying pathological processes.

Assuming the tripartite nature of central nervous system synapses [32] it is possible that the astrocytic dysfunction, compromising the neuronal activity support and/or gliotransmission, disturbs synaptic transmission and plasticity or neuronal excitability. These events at the cellular level are translated into distortion of brain physiology that lead to behavioural abnormalities [38]. Rat models of depression exhibit decreasing levels of GFAP expression and ^{13}C -acetate metabolism reflecting glial metabolism [75, 77]; also in rat, glial loss in the prefrontal cortex (PFC) is sufficient to induce depressive-like behaviour [76]. In the context of epilepsy, GFAP immunoreactivity evidenced astrocytic hypertrophy (reactive astrocytosis) and proliferation [78]: in mesial temporal lobe epilepsy, GFAP immunoreactivity is increased in a way that might be correlated with seizure frequency [79]. Moreover, astrocytic Ca^{2+} oscillations were observed to increase in frequency in isolated brain slice models that exhibit epileptiform activity [80]. However, while enhanced excitatory gliotransmission, for example in terms of Ca^{2+} oscillations and glutamate release, can contribute to epileptiform activity and seizures, reduced gliotransmission and D-serine release can contribute to schizophrenia. Also contrasting is the decreased GFAP expression in tissue isolated from schizophrenic patients [81-83]. In Alzheimer's disease, increased levels of amyloid- β ($\text{A}\beta$) peptides and their subsequent deposition in $\text{A}\beta$ plaques lead to the activation of the surrounding microglia and astrocytes that release diverse pro- and anti-inflammatory mediators resulting in the chronic parenchymal inflammation in the brain [84, 85]. In Parkinson's disease, and other neurological disorders, occurs an abnormal neuronal aggregation of α -synuclein, that is directly transmitted from neurons to astrocytes, causing inflammatory responses [86]

1.3. Astrocytic function in vivo: behaviour and cognition

The discovery that astrocytes respond to neuronal transmitters through Ca^{2+} elevations [87, 88] have boosted the studies on astrocytic function attempting to understand more about the implications of these glial cells in brain activity and its output. Initially, the research tools limited the scientific progress on this subject, but successive studies have been giving input for a new insight into the role of glial in the brain function.

Functional and metabolic studies with toxins targeting selectively astrocytes have provided simple approaches to study the effects of astroglial dysfunction. Intracerebral injections of the gliotoxin L- α -aminoadipate, caused the disruption of the astrocytic network when injected intracerebrally in Long Evans Hooded and Sprague Dawley rats, since it irreparably damaged the astrocytes in the vicinity of injections [89]. Using this model of glial loss, Banasr and colleagues were able to induce depressive-like behaviour in rats [77].

Additionally, a recent study proved that astrocytes modulate the accumulation of sleep pressure and its cognitive consequences. These conclusions were achieved using the dnSNARE transgenic mice model that conditionally prevents astrocyte-dependent action on pre-synaptic A1 receptors through the conditional blockade of vesicular release. Because adenosine is involved in homeostatic drive of sleep following prolonged wakefulness, sleep pressure was significantly reduced when dnSNARE transgene was expressed in astrocytes [47]. Another study based in the same animal model followed with the evidence that astrocytic-derived ATP acting on A1 receptors via adenosine contributes to the effects of sleep deprivation on hippocampal plasticity and hippocampus-dependent memory [90].

Although these studies unveil a putative role of astrocytes in the regulation or modulation of behaviour outputs much more in this field should be cleared. By implementing different animal models of astrocytic dysfunction we expect to assess the implications of astrocytic function in the generation or modulation of cognitive function.

1.4. The prefrontal cortex

In this project we focused in the cognitive function and we focused in the prefrontal cortex because (1) it is a region with major relevance for cognitive processes (see section 1.4.1), (2) it is a large region in the brain, and therefore relatively easy to target for injections of pharmacological tools (aminoadipate rat model, see section 3.1.1)

1.4.1. Cognitive functions of the the prefrontal cortex: learning and memory

The prefrontal cortex (PFC), which is among the most studied regions of the brain, is intimately related to the computation of complex cognitive functions. Indeed, various cognitive and executive processes have been associated to the PFC, such as working memory, decision making, planning and behavioural flexibility, attentional set-shifting and inhibitory response control [91, 92]. The PFC has been shown to be implicated in the organisation of delayed responses and consequently in working memory function - a memory system composed of distinct, but overlapping cognitive processes used for the active maintenance and elaboration of task-relevant information, as it involves temporary storage and manipulation of information [93]. Functional neuroimaging in brain-damaged humans and healthy volunteers have confirmed the role of the PFC in working memory processes [94]. Neuropsychological and connectional evidences indicate the homology of the medial prefrontal cortex (mPFC) in rats and the dorsolateral prefrontal cortex (dlPFC) in primates. [95-98] - fig. 1.5. As the dlPFC in primates, the mPFC in rats is involved in other executive functions, besides working memory: temporal organisation of behaviour [99] and attentional control in strategy switches [98, 100, 101]. In fact, lesions in the rat mPFC - prelimbic (PrL), infralimbic (IL), and with partial damage to the cingulate cortex areas 1 and 2 (Cg1 and Cg2) - impair selectively the extradimensional set-shifting [98]. Moreover, the rat mPFC was proposed to be important in the representation of an abstract and more hierarchically-organised memory useful in the decision making, complementing the hippocampus in spatial navigation [102]. It is not surprising, since the IL and PrL regions of the PFC, constituting the ventral portion of the rat mPFC, are linked to the hippocampus by an axonal pathway originated in the subiculum and ventral CA1 [103].

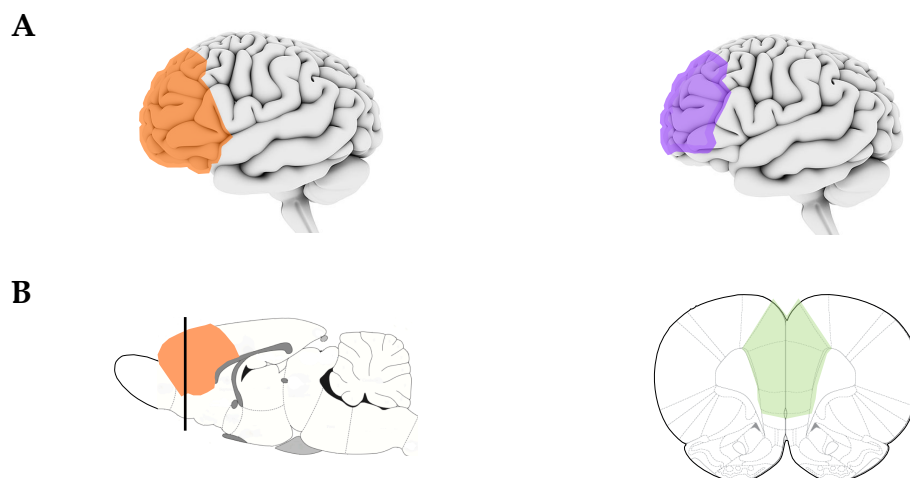


Figure 1.5. Highlights of the PFC and mPFC, in human brain evidencing the homology of mPFC and dlPFC brain regions in rat and human, respectively [92]. A - lateral view of human brain; and B, left - sagittal view of rat brain; B, right coronal section at Bregma 3.0. Orange PFC Purple dlPFC Green mPFC

2. AIM OF WORK

The rationale of this project is based in the common accepted idea that specific brain regions compute specific tasks and are responsible for specific behavioural outputs. In this scope, we believe that affecting the astrocytic function in a brain region, mimicking what happens in pathological states [75-85], and measuring the behaviour output of that region we would be able to dissect the astrocytic component of that behaviour output.

Despite the many years of research carried out so far in the astroglial function in the brain, most of these studies were focused on metabolic and physiologic features and little was done in what concerns to behaviour implications, namely in cognitive function, involving learning and memory, in the context of altered astrocytic function.

The aim of this work is to implement two animal models whose astrocytes are affected in two different manners to allow in vivo study of astrocytic function and its implication in behaviour outputs. Hence, (1) to mimic pathologies based on the glial loss we implemented a rat model on which astrocytes were ablated through the gliotoxin L- α -aminoadipate; and (2) to disclose the role of the exocytotic release of gliotransmitters in cognitive processes, we implemented the recently reported genetic mouse model, dnSNARE.

In this project we focused in the cognitive function linked to the prefrontal cortex because (1) it is a region with major relevance for cognitive processes (see section 1.4), (2) it is a large region in the brain, and thus relatively easy to target for injections of pharmacological tools (aminoadipate rat model). By lesioning astrocytes in the mPFC and blocking the gliotransmitter release by astrocyte we expect to observe a compromise in learning and memory functions mostly dependent on the PFC and therefore dissect the astrocytic component in the computation of these tasks.

3. MATERIALS AND METHODS

3.1. *Animals and Treatments*

Experiments were conducted in accordance with local regulations (European Union Directive 86/609/EEC) and National Institutes of Health guidelines on animal care and experimentation.

3.1.1. *Amino adipate rat model of astrocytic depletion*

Male Wistar-Han rats (Charles River Laboratories, Barcelona, Spain), ten-weeks-old, were housed in groups of two, under standard laboratory conditions (room temperature 22°C; food and water *ad libitum*; 12h dark/light cycle, lights on at 8:00 AM). One group was subjected to pharmacological ablation of astrocytes in the mPFC through a single bilateral intracerebral microinjection of the selective astrocytic toxin L- α -amino adipate (L- α -AA; see section 3.1.1.B) - treatment group (AA). As control animals (CON) for the amino adipate pharmacological model, other set of rats received a single bilateral intracerebral microinjection of artificial cerebrospinal fluid (aCSF), the vehicle of the amino adipate solution, in the same region, using the same procedure.

3.1.1.A. *Surgical procedure for the establishment of the pharmacological rat model*

For the establishment of the amino adipate pharmacological model, rats were subjected to a surgical procedure for the implantation of bilateral cannula guides in the prelimbic region of the prefrontal cortex. Animals were deeply anaesthetised with a intraperitoneal (i.p.) mix of ketamine (75 mg/kg - Imalgene 1000, Merial) and medetomidine (0,5 mg/kg - Dorbene Vet, Pfizer) and bilateral brain cannulas (26 GA, Plastics One) were stereotaxically implanted in the prelimbic region of the prefrontal cortex. The coordinates used were: 3.0 mm posterior to bregma, \pm 0.6 mm lateral to the midline, and 2.5 mm ventral to the skull surface, based on the Paxinos and Watson rat brain atlas [104]. This position represents a spot 1 mm above the target position, which will be achieved by the internal cannulas, used to inject the solution of interest. The fixation of the bilateral cannula guides in the skull was achieved by the placement of two screws in anterior and posterior positions to relative to the cannula, and by the application of an acrylic resin (Pattern Resin LS, GC) covering both screws and the basal portion of the cannula guide pedestal. At the end of the surgical procedure the anaesthesia

was reverted with atipamezol, i.p. (2 mg/kg - Antisedan, Pfizer) and animals were housed individually to avoid damage of the implant. Animals were allowed to recover from this surgical procedure for at least 7 days.

3.1.1.B. Drug preparation and administration

A 124 mM L- α -aminoadipate drug solution was prepared through the solubilisation in aCSF as previously described [89], by simply dissolve L- α -aminoadipate (A7275, Sigma-Aldrich) in aCSF and adjusting the pH to 7.4 in order to help to dissolve the aminoadipate.

Concerning the drug infusion protocol, rats were first anaesthetised with mix of propofol (70 mg/kg - Vetofol, Esteve) and medetomidine (0,2 mg/kg - Dorbene Vet, Pfizer) administered intraperitoneally. Such anaesthesia protocol based on Alves et al, 2010 provides suitable level of sedation ideal for restraint and non-painful drug infusion [105]. Five microliters of AA (620 μ mol), or aCSF were administered using 25 μ l Hamilton syringes, connected to a double internal cannula (that projects 1 mm from the cannula guide) through a polyethylene tubing, at the constant rate of 0.5 μ l/min controlled by an micro-pump (53100V, Stoeling). The double internal cannula was slowly withdrawn 5 minutes after infusion completion to avoid the displacement of the injected fluid by capillarity. Once this procedure was complete, anaesthesia was reverted with atipamezol (1 mg/kg - Antisedan, Pfizer) and animals returned to their home-cages.

As the selective gliotoxin L- α -aminoadipate exerts effect 4 hours following injection [89] and the astrocyte ablation effect persists up to 7 days, this drug was infused in the rats brains on the day before the behaviour tests. In this way, rats preformed the behaviour tests within the window of time of L- α -aminoadipate effect.

3.1.2. Transgenic dominant-negative SNARE mice (dnSNARE) genetic model

For the purpose of this project we obtained the dnSNARE transgenic mice strain from Prof. Philip Haydon (Tufts University, Boston) that kindly supplied the founders, and implemented the colony at the IVCS. In this strain the SNARE domain of the synaptobrevin II (dnSNARE) expression is conditionally suppressed in astrocytes, by means of a “tet-Off” expression system. The dnSNARE mice strain was generated by Pascual and colleagues [106], by expressing the cytosolic portion of the SNARE domain of synaptobrevin II (amino acids 1 to 96) selectively in GFAP-positive astrocytes, which blocks the exocytotic release of

gliotransmitters, a process dependent on the formation of SNARE complexes [107]. For that purpose, they developed two separate mice lines GFAP.tTA and tetO.dnSNARE that when crossed yield dnSNARE mice. The GFAP.tTA mice line contains the astrocyte-specific glial fibrillary acidic protein (GFAP) promoter that drives the expression of the tetracycline-controlled transactivator protein (tTA), while the tetO.dnSNARE mice line contains a SNARE domain regulated by a tet operator promoter (tetO) and the reporter gene enhanced green fluorescent protein (EGFP) - fig. 3.1.

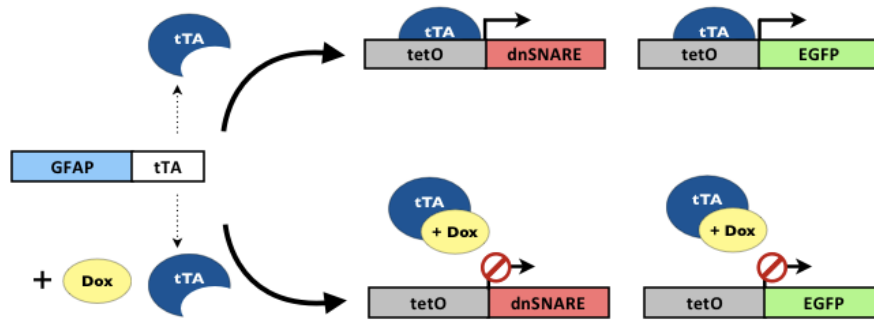


Figure 3.1. Schematic representation of GFAP promoter driving the expression of the target gene dnSNARE and reporter gene EGFP in astrocytes. Tetracycline doxycycline (Dox) suppresses the expression of transgenes by preventing the binding of tTA to tetO. Adapted from Florian *et. al*, 2011 and Halassa *et. al*, 2009 [40, 90]

3.1.2.A. Colony implementation: strain lines and matings

To implement this transgenic mice strain in the ICVS, the two mice lines GFAP.tTA and tetO.dnSNARE, were first maintained heterozygous under C57/Blk6 genetic background. Mice originated by the backcrosses of those two separate lines were crossed (GFAP.tTA x tetO.dnSNARE) to produce dnSNARE mice for experimentation. The double negative and single positive offspring were kept as controls. In the GFAP-positive astrocytes of these animals the expression of transgenes SNARE, LacZ and EGFP is suppressed by the tetracycline doxycycline (Dox). To prevent potential developmental effects of the transgene expression, mice were bred and raised until weaning, at three weeks of age, under the action of Dox (Sigma, 25 µg/ml in drinking water). Once animals were weaned, Dox administration was maintained until 3 weeks prior to the behavioural studies. Transgene-expressing and wild type mice were visually indistinguishable [106]. The double negative, single and double positive offspring were tested in behaviour paradigms described below (see sections 3.2.2).

3.1.2.B. *Colony management and genotyping*

In the context of colony management, the genotyping of the offspring generated by the matings was accomplished by means of polymerase chain reaction (PCR) of DNA extracted from mice tails (about 3 mm of the tip). First, the tails were digested in 380 µl of cell lysis buffer (0,5 mM Tris, pH 8.0; 10 mM EDTA; 0,5 % SDS) with 10 µl of proteinase K (15 mg/ml), overnight and in a heating block at 55°C. In the next morning, samples were centrifuged during 10 minutes at 13000 rpm and the supernatant was collected. The DNA precipitation was achieved by the addition of 300 µl of isopropanol to the collected supernatant, followed by soft shaking of the sample tubes. After additional 10 minutes centrifugation at 13000 rpm, the supernatant was discarded, while the pellet was rapidly washed with 100 µl of ethanol 70%. The tubes containing the DNA sample were then left air drying at the bench for 90 minutes, after which DNA hydration was attained by the addition of 50 to 100 µl of elution buffer (10 mM Tris, pH 8.0; 1 mM EDTA) and a short vortex.

The genotyping itself was then carried out by the multiplex PCR technique, on which the two pairs of primers, for tTA (tTA forward: 5'- ACT CAG CGC TGT GGG GCA TT - 3'; tTA reverse: 5' - GGC TGT ACG CGG ACC CAC TT - 3') and tet.O (tet.O forward: 5'- TGG ATA AAG CTC ATT AAT TGT CA - 3'; tet.O reverse: 5' - GCG GAT CCA GAC ATG ATA AGA - 3') sequences, were used in the same PCR mixture. The PCRs were performed in a MyCycle thermal cycler (Bio-Rad); the composition of the PCR mix and conditions used are summarised in the table 3.1. Amplified PCR products were separated on a 1% agarose gel prepared in Tris-Acetate-EDTA (TAE) running buffer, stained with ethidium bromide and compared to the DNA size marker GeneRuler™ 1kb Plus DNA Ladder, 75-20,000bp (#SM1331, Fermentas). Electrophoresis run for 40 minutes at 120V and gel images were captured with a transilluminator (Alpha Innotech Corporation, Bio-Rad).

Table 3.1. PCR conditions used for the amplification of tTA and tet.O sequences.

Reaction mix (20 μ l) components		
Taq buffer, with KCl (part of #EP0402, Fermentas)		1x
MgCl ₂ (part of #EP0402, Fermentas)		1.5 mM
dNTP mix (#R0192, Fermentas)		0.2 μ M
Primer tTA forward		0.5 μ M
Primer tTA reverse		0.5 μ M
Primer tet.O forward		0.5 μ M
Primer tet.O reverse		0.5 μ M
Taq DNA Polymerase (#EP0402, Fermentas)		0.5 U
DMSO		2%
Template DNA		100 ng

Amplification program		
Step	Temperature ($^{\circ}$ C)	Duration (sec)
Initial denaturation	94	180
Denaturation	94	45
Annealing	61.2	60
Extension	72	60
Final extension	72	600

3.2. Behaviour Tests

3.2.1. Amino adipate rat model of astrocytic depletion

The behavioural consequences of astrocyte depletion in the medial prefrontal cortex, induced by intracranial injection of L-amino adipate (see section 3.1.1) were assessed by the attentional set-shifting task and by water maze-based tests. These tests were used to measure the cognitive performance of animals with astrocytic depletion and the respective controls, and are described in detail below.

3.2.1.A. Attentional set-shifting task

To assess the non spatial working memory, the attentional set-shifting and the reversal learning of rats subjected to the intracranial bilateral injections of AA we used the attentional

set-shifting task (ASST). The protocol of this cognitive test was adapted from the ASST paradigm originally described by Birrell and Brown [98]. The task was conducted in a custom made black Plexiglass apparatus (60 cm L x 40 cm W x 20 cm H). One third of the apparatus was separated by the rest of the area by a removable divider, creating a holding area. On the opposite side, two adjacent plastic pots filled with sawdust, separated by a vertical divider, were used as digging bowls and their rims were scented with different oil essences, producing a lasting odour - fig. 3.2.

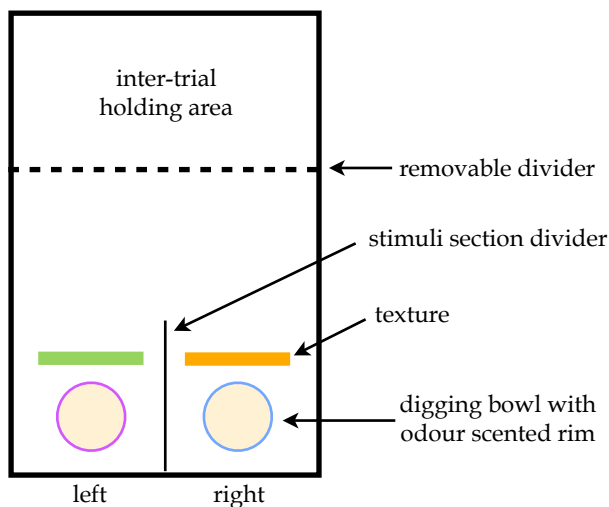


Figure 3.2. Representation of the ASST apparatus. The combinations of stimuli are located in one third of the apparatus area divided in two sections, where the stimuli combinations are presented at each trial. The opposite third of apparatus separated by a removable divider constitutes a holding area where the rat rests between trials.

In each trial the pot associated with the correct answer contained a small food reward (Nestle Cheerio ring cut in two parts) buried underneath the digging media, as rats could be trained to dig in small bowls filled with sawdust to retrieve food reward [108]. The reward was predicted either by an odour in the bowl or by a different texture before reaching the bowl. Because this test involves a food reward to correct answers, all animals were food restricted (1 h of access to food per day) during the prior 6 days. During this food restriction period, 6 Nestle Cheerios were given to the rats per home cage. The task was conducted in a room with dim light, controlled by a rheostat. Animals were brought to the test room 15 minutes before its start, to acclimatise them to those room conditions.

On the two days before the test animals were acclimatised to the apparatus, with food rewards in both digging bowls, for 1 hour each day. On the day 1 of the task animals have to discriminate from one stimulus, while on the day 2 of the task the animals are presented with 2 different dimensions of stimuli, odours or textures and have to learn which stimulus leads

to the reward. On the day 1 of the task, after 5 minutes of habituation to the apparatus, animals were first trained in two stages of simple discrimination (SD): odours (lemon vs. vanilla)- SDO- and textures (sandpaper vs. blue plastic)- SDT. The second day of the task consisted of compound discrimination of odours- CDO- (papaya vs. eucalyptus and cardboard vs. brown plastic), reversal compound discrimination- Rev1; extradimensional shift- EDST- (mango vs. lotus and velvet vs. plastic grass); and reversal extradimensional shift- Rev2. In the reversal stages, the previous positive stimulus, i.e. associated with the reward, became negative - table 3.2. The stages were only completed when the animals reached 6 correct consecutive trials- when it is considered that the animal learned to associate the positive stimulus to the reward [98]- apart from the first 2 trials, when animals are allowed to freely explore the both digging bowls. Stimuli were presented in a random sequence of 10 trials (equal to all animals), repeated if necessary - tables 3.3, 3.4 and 3.5. As in task day 1, animals were allowed to habituate to the apparatus during 5 minutes.

Once task was completed animals returned to their home cages, remaining at that same room until sacrifice.

Table 3.2. Order of discrimination stages, relevant and irrelevant dimensions, and stimuli combinations of ASST presented to the animals. Reward associated stimuli are bold and minus sign indicates absence of stimulus.

Discrimination Stages	Dimensions		Stimuli combinations	
	Relevant	Irrelevant	Positive	Negative
Odor Simple Discrimination(SDO)	Odor	-	Lemon	Vanilla
Texture Simple Discrimination (SDT)	Texture	-	Sandpaper	Blue Plastic
Compound Discrimination (CD)	Odor	Texture	Papaya /Eucalyptus	Cardboard/Brown Plastic
Reversal Compound Discrimination (Rev1)	Odor	Texture	Papaya / Eucalyptus	Cardboard/Brown Plastic
Extradimensional Shift (EDST)	Texture	Odor	Velvet /Plastic Grass	Mango/Lotus
Reversal Extradimensional Shift (Rev3)	Texture	Odor	Plastic Grass /Velvet	Mango/Lotus

Table 3.3. Stimuli combinations and sequence of presentation along 10 trials of the simple discrimination, stages on test day one: simple discrimination of odors (SDO) and simple discrimination of textures (SDT). Reward associated stimuli are bold and minus sign indicates absence of stimulus; the shading highlights the position of the stimulus in the test apparatus.

Stage	SDO				SDT				
	Right		Left		Right		Left		
	Trial	Odor	Texture	Odor	Texture	Odor	Texture	Odor	Texture
1	Lemon	-		Vanilla	-	-	Sandpaper	-	Blue Plastic
2	Vanilla	-		Lemon	-	-	Sandpaper	-	Blue Plastic
3	Lemon	-		Vanilla	-	-	Blue Plastic	-	Sandpaper
4	Vanilla	-		Lemon	-	-	Blue Plastic	-	Sandpaper
5	Lemon	-		Vanilla	-	-	Sandpaper	-	Blue Plastic
6	Vanilla	-		Lemon	-	-	Blue Plastic	-	Sandpaper
7	Vanilla	-		Lemon	-	-	Blue Plastic	-	Sandpaper
8	Vanilla	-		Lemon	-	-	Sandpaper	-	Blue Plastic
9	Lemon	-		Vanilla	-	-	Sandpaper	-	Blue Plastic
10	Lemon	-		Vanilla	-	-	Blue Plastic	-	Sandpaper
Reward: <i>Lemon</i>					Reward: <i>Sandpaper</i>				

Table 3.4. Stimuli combinations and sequence of presentation along 10 trials of the test first compound discrimination and its reversal stages: compound discrimination of odors (CDO) and reversal stage one (Rev1). Reward associated stimuli are bold; the shading highlights the position of the stimulus in the test apparatus.

Stage	CDO				Rev1				
	Right		Left		Right		Left		
	Trial	Odor	Texture	Odor	Texture	Odor	Texture	Odor	Texture
1	Papaya	Brown Plastic		Eucalyptus	Cardboard	Papaya	Cardboard	Eucalyptus	Brown Plastic
2	Eucalyptus	Brown Plastic		Papaya	Cardboard	Papaya	Cardboard	Eucalyptus	Brown Plastic
3	Eucalyptus	Cardboard		Papaya	Brown Plastic	Papaya	Cardboard	Eucalyptus	Brown Plastic
4	Eucalyptus	Cardboard		Papaya	Brown Plastic	Eucalyptus	Cardboard	Papaya	Brown Plastic
5	Papaya	Cardboard		Eucalyptus	Brown Plastic	Eucalyptus	Brown Plastic	Papaya	Cardboard
6	Papaya	Brown Plastic		Eucalyptus	Cardboard	Papaya	Brown Plastic	Eucalyptus	Cardboard
7	Eucalyptus	Brown Plastic		Papaya	Cardboard	Eucalyptus	Brown Plastic	Papaya	Cardboard
8	Eucalyptus	Cardboard		Papaya	Brown Plastic	Eucalyptus	Cardboard	Papaya	Brown Plastic
9	Papaya	Cardboard		Eucalyptus	Brown Plastic	Papaya	Brown Plastic	Eucalyptus	Cardboard
10	Papaya	Cardboard		Eucalyptus	Brown Plastic	Eucalyptus	Brown Plastic	Papaya	Cardboard
Reward: <i>Papaya</i>					Reward: <i>Eucalyptus</i>				

Table 3.5. Stimuli combinations and sequence of presentation along 10 trials of the test second compound discrimination and its reversal stages: extradimensional shift- discrimination of textures- (EDST) and reversal stage two (Rev2). Reward associated stimuli are bold; the shading highlights the position of the stimulus in the test apparatus.

Stage	EDST				Rev2			
	Right		Left		Right		Left	
Trial	Odor	Texture	Odor	Texture	Odor	Texture	Odor	Texture
1	Lotus	<i>Velvet</i>	Mango	Plastic Grass	Lotus	Velvet	Mango	<i>Plastic Grass</i>
2	Mango	Plastic Grass	Lotus	<i>Velvet</i>	Mango	Velvet	Lotus	<i>Plastic Grass</i>
3	Mango	<i>Velvet</i>	Lotus	Plastic Grass	Lotus	Velvet	Mango	<i>Plastic Grass</i>
4	Mango	<i>Velvet</i>	Lotus	Plastic Grass	Lotus	<i>Plastic Grass</i>	Mango	Velvet
5	Lotus	Plastic Grass	Mango	<i>Velvet</i>	Lotus	Velvet	Mango	<i>Plastic Grass</i>
6	Lotus	Plastic Grass	Mango	<i>Velvet</i>	Mango	Velvet	Lotus	<i>Plastic Grass</i>
7	Mango	Plastic Grass	Lotus	<i>Velvet</i>	Mango	<i>Plastic Grass</i>	Lotus	Velvet
8	Mango	Plastic Grass	Lotus	<i>Velvet</i>	Mango	<i>Plastic Grass</i>	Lotus	Velvet
9	Lotus	<i>Velvet</i>	Mango	Plastic Grass	Mango	Velvet	Lotus	<i>Plastic Grass</i>
10	Lotus	<i>Velvet</i>	Mango	Plastic Grass	Lotus	<i>Plastic Grass</i>	Mango	Velvet
Reward: <i>Velvet</i>				Reward: <i>Plastic Grass</i>				

3.2.1.B. Water maze tests

The tests were conducted in a circular black pool (170 cm diameter) filled with water at 22°C to a depth of 34 cm in a room with extrinsic clues (triangle, square, cross and horizontal stripes) and rheostat controlled dim light. Imaginary lines were dividing the tank in four quadrants, one of which containing a submerged cylindrical plexiglass platform (12 cm, 32 cm high) covered with black plastic to remain un distinguishable from the pool - fig. 3.3 . Rats behavioural data was collected by a video camera fixed in the ceiling and connected to a video-tracking system (Viewpoint, Champagne au mont d'or, France). The water maze tests consisted of a six days protocol and involved four distinct tasks. In general, the tasks are composed by four trials with the maximum duration of 2 minutes. At the beginning of each trial rats were placed in the water facing the maze wall and oriented to one of the four extrinsic clues, i. e., in one of the four imaginary quadrants (Q1, Q2, Q3 and Q4). The trial was only complete when the animal escaped to the platform or in case the animal did not reach the platform two minutes after the beginning of the trial. In that case, animals were gently guided to the platform. After twenty seconds on the platform, rats were then taken out of the maze to start a new trial. At the end of each trial the distance swam and escape latency were registered. In the cases when rats did not find the platform, the registered escape latency was 2 minutes (120 seconds) .

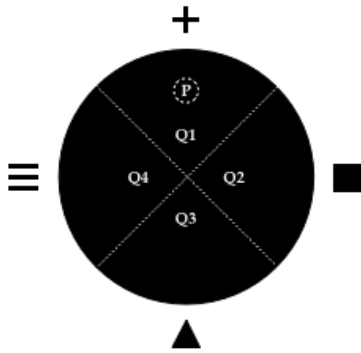


Figure 3.3. Representation of the water maze tests apparatus, prepared for rats with the extrinsic clues (triangle, square, cross and horizontal stripes) and the platform (P). Four imaginary quadrants (Q1, Q2, Q3 and Q4) divided the pool.

Working memory task (WMT): The first of the paradigms used was the working memory task, a variant of the spatial reference memory test [109] to assess this PFC function. The purpose of this task is to assess the ability of rats to learn the location of the hidden platform and to retain this information online during the four consecutive trials. Usually, the working memory task consists of four days. At each day the platform location is the same in all four trials, but varies from day to day using a different quadrant per day [99]. Considering that the aminoacidate model of astrocytic dysfunction has a window of time of only seven days to perform behaviour tests we decided to remove one of the days from this task just to be sure that animals were performing the tests with the aminoacidate effect-window. We chose to remove the day on which the first trial of the task is started in the same quadrant of the platform. Average escape latencies and distance swam in each trial along the three days of this task were considered as working memory test results, since faster animals display better working memory performance.

Spatial reference memory task (RMT): following the working memory task (days 1-3) animals performed the reference memory task, which is hippocampus-dependent [109], until day 5 (the first day of working memory task was also considered as the first day of reference memory task and the last day of working memory task was also considered as the second day of the reference memory task). On this task, the platform was kept in the same quadrant as test in day 3 so that we could assess the ability of the animals to learn the position of the platform along the days. The escape latencies and distance swam output of this test were analysed as means from the four trials of each day and interpreted as reference memory performances. Animals with shorter latencies or distance swam display better reference memory.

Reversal learning task (RLT): On day 6, the animals performed the reversal learning task, which is prefrontal cortex-dependent [110], on which the platform is placed in the opposite quadrant of the previous location learnt in the reference memory task. The reversal learning of the rats was evaluated through the analysis of the distance swam and time spent in each

quadrant as a mean of the four trials. An extra trial, probe trial, in which the platform is removed from the tank, was performed to confirm that the reversal learning was correctly executed [109]. During the 2 minutes of this probe trial the distance swam and time spent in each quadrant were measured. A good performance in the reversal learning consisted of higher percentage of time or distance swam in the new quadrant, when compared to the old quadrant.

The timeline followed in this cognitive test with the rat model of astrocytic ablation is depicted in table 3.6.

Table 3.6. Timeline followed in the water maze tests used for rat models of astrocytic ablation.

Task	WMT 1/ RMT 1	WMT 2	WMT 3/ RMT 2	RMT 3	RMT 4	RLT + Probe
Day	1	2	3	4	5	6

3.2.2. *dnSNARE mice model of impaired vesicular release in astrocytes*

The dnSNARE mice were recently created [106] and the behaviour phenotype of this mice strain is still poorly tested [40] (see chapter 5). Therefore we performed primarily the open field test and the elevated plus maze to assess if these animals possess any lack of exploratory motivation, locomotion difficulties or anxiety that would mislead us in tests that measure cognition. Then the animals were tested in water maze-based paradigms and in the continuous spontaneous alternation test to assess cognitive function. Details on the specific tests are given below.

3.2.2.A. Elevated Plus Maze (EPM)

The paradigm of this test was established by Hanldy and Mithani [111] basing in the observations that elevated open alleys evoke greater avoidance responses than closed alleys in rat [112] and was already validated also for the use in mice [113]. dnSNARE mice anxious phenotype was assessed in a “plus” shaped maze (ENV-560, Med Associates, Inc.) consisting in two opposite open arms (50.8 cm L x 10.2 cm W x 40.6 cm H) and other opposite closed arms (50.8 cm L x 10.2 cm W x 40.6 cm H), elevated 72.4 cm above the floor. During the 5 days prior to the test, mice were handled once a day for 1 minute each. Mice exploratory activity in the EPM was individually recorded during 5 minutes and the time spent in open

arms, hub (arms junction area) and the number of entrances and explorations in each section were analysed through a system of infrared photo-beams using a video tracking interface (SOF-842, Med Associates, Inc.). The test was performed under bright white light. The maze was carefully cleaned, between each animal, with 10% ethanol to avoid traces to be left from one animal to another. The collected data was used to calculate the ratio of time spent in open arms over time in closed arms and the percentage of open arms entries, being time presented as percentage over total duration of the trial.

3.2.2.B. Open field test (OF)

In order to assess the spontaneous locomotor activity, exploratory behaviour and anxiogenic-like behaviour (thigmotaxis) [114-116] in dnSNARE mice, the OF test was used. Mice were handled for 1 minute each day during 5 consecutive days before the test. The test was conducted in a Plexiglass box enclosing a white arena (43.2 cm L x 43.2 cm W x 30.5 cm H) with a centre zone delimited with an imaginary perimeter set at 10 cm from the sides of the arena (ENV-515-16, Med Associates, Inc.). Total distance moved (length of the path), movement speed, number of rearings and time spent in the centre zone were analysed through the 16 infrared photo-beams using Activity Monitor video tracking system (SOR-811, Med Associates, Inc.). At the beginning of the test session, mice were placed individually into the middle of the OF arena and let explore during 5 minutes. Between each animal, the arena was carefully cleaned with 10% ethanol to avoid traces to be left from one animal to another.

3.2.2.C. Water maze tests

The water maze tests were conducted in a circular white pool (170 cm diameter) filled with water at 22°C to a depth of 32 cm in the same room as rats water maze tests with the extrinsic clues (triangle, square, cross and horizontal stripes) and rheostat controlled dim light, similarly to the one used to test the rat animal model. Imaginary lines were dividing the tank in four quadrants, one of which containing a cylindrical plexiglass platform (8 cm, 30 cm high) - fig 3.4. Mice behaviour data was collected with a video camera fixed in the ceiling and connected to a video-tracking system (Viewpoint, Champagne au mont d'or, France). The water maze tests consisted in a five days protocol that involved two distinct tasks: reference memory task and reversal task. Similarly to the protocol used for rats water maze tests, in general tasks are composed by four trials with the maximum duration of 2 minutes. At the beginning of each trial mice were placed in the water facing the maze wall

and oriented to one of the four extrinsic clues, in one of the four imaginary quadrants (Q1, Q2, Q3 and Q4). The trial was complete when the animal escaped to the platform or when the escape did not occur within 2 minutes. In that case, mice were gently guided to the platform. After twenty seconds on the platform, mice were taken out of the maze to start a new trial. At the end of each trial the distance swam and escape latency was registered. In the cases when mice did not find the platform, the registered escape latency was 2 minutes (120 seconds).

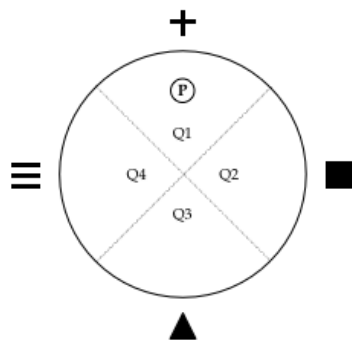


Figure 3.4. Representation of the water maze tests apparatus, prepared for mice, with the extrinsic clues (triangle, square, cross and horizontal stripes) and the platform (P). Four imaginary quadrants (Q1, Q2, Q3 and Q4) divided the pool.

Spatial reference memory task (RMT): mice were tested for its spatial reference memory with the hippocampus-dependent reference memory task [109], until day 4. On this task, the platform was kept in the same quadrant so that we could assess the ability of mice to learn the position of the platform along the four days. The escape latencies and distance swam output of this test were analysed as means from the four trials at each day and interpreted as reference memory test. Animals with shorter latencies or distance swam display better reference memory.

Reversal learning task (RLT): The PFC function was assessed by the reversal learning task on which the platform is placed in the opposite quadrant of the previous location [110], similarly to the procedure for rats. The reversal learning of the mice was evaluated through the analysis of the distance swam and time spent in each quadrant as a mean of the remaining three trials, with a duration of 2 minutes each. A good performance in the reversal learning consisted of more percentage of time or distance swam in the new quadrant, when compared to the old quadrant.

The timeline followed in this cognitive test for the mice model of astrocytic dysfunction is specified in table 3.7.

Table 3.7. Timeline followed in the water maze tests used for the mice models of astrocytic dysfunction.

Task	RMT				RLT
Day	1	2	3	4	5

3.2.2.D. Continuous spontaneous alternation test

This test, conducted in Y-maze, was used to assess spatial working memory function in transgenic dnSNARE mice. The Y-maze apparatus consisted of three costume made white Pexiglass closed arms (35 cm L x 5 cm W x 8 cm H), elevated x 120 cm above the floor, based on published protocols previously adapted for mice [117, 118]. Each arm is identical, so that intra-maze cues were not provided to mice, while they were allowed to see distal spatial landmarks (triangle, horizontal stripes and cross). The test was performed by placing each mouse in the centre (c) of the three arms of the apparatus and letting the animal to explore the maze freely during 5 minutes - fig3.5. A video camera was used to record the movements of the animal in the maze. This test is based on innate curiosity of rodents to explore novel areas, which is relies in their working memory. This test presents no negative or positive reinforcements, therefore not stressful for the animals. The number and sequence of arm entrances was recorded manually. The total of number of arm entrances was used as a measure of motivation to explore the maze and locomotor activity. The assessment of mice spatial working memory was given by the percentage of alternations (alternation score, %) was calculated, basing on the principle that one alternation was counted when animals visited the three different arms consecutively and immediate reentries were discounted (for example, 1-3-2; 2-1-3). The assessment of mice spatial working memory was given by the percentage of alternations (alternation score, %), being one complete alternation each time the animal visited the three different arms consecutively (immediate reentries were discounted). The alternation score was calculated by the number of alternations divided by the total possible alternations (number of arms entered minus 2) and multiplied by 100 [117].

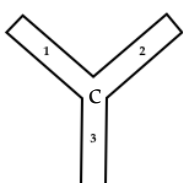


Figure 3.5. Representation of the Y maze apparatus. The 3 arms are randomly numbered from 1 to 3; c - centre of the Y-maze.

3.3. *Histological procedures*

3.3.1. *Euthanasia and tissue preparation*

One hour after ASST or water maze tests completion rats were deeply anaesthetised with an overdose of ketamine and medetomidine mix, and readily perfused transcardially with ice cold paraformaldehyde 4% in PBS (0.1 M, pH 7.4) solution. Brains were then removed and placed in the same fixative for 48 hours and then in 30% sucrose in PBS solution (for impregnation) until sinking, at 4°C under agitation. Once sunked, brains were frozen by immersion in liquid nitrogen in Neg-50 frozen section medium (Thermo Scientific) and stored at -80°C until sectioning. The tissue obtained represented the lesion of amino adipate at day 3 and day 7 post-injection, whether the animals had performed the ASST or water maze-based tests, respectively.

3.3.2. *Immunofluorescent staining of astrocytes and neurons*

In order to analyse the histological implications and extension of the lesion caused not only by the injection of AA, but also by the mechanical trauma of the bilateral cannula guides implantation, we performed the immunofluorescent detection of astrocytes and neurons in 20 µm thick coronal sections of the PFC cut in a cryostat (Leica CM1900). The immunofluorescent procedures were only applied to representative brain sections, selected by signs of cannula entry at the brain surface.

For the immunofluorescent detection of neurons and astrocytes, the procedure started with an antigen retrieval step, with citrate buffer (10 mM) during 20 minutes at 100W microwave potency. Once cooled, slices were submitted to two rinses of 3 minutes in PBS, followed by the overnight incubation with the primary antibodies rabbit polyclonal anti-rat GFAP (1:200, DakoCytomation) and mouse polyclonal anti-rat NeuN (1:100, Milipore) in PBS with 0,5% Triton X-100 and 10 % fetal bovine serum (FBS). After three rinses of 3 minutes in PBS, sections were then incubated with the secondary antibodies Alexa Fluor® 594 goat anti-rabbit and Alexa Fluor® 488 goat anti-mouse (1:1000, Molecular Probes®) in PBS with 0,5% Triton-X, during 90 minutes. Once slices were rinsed again, the cellular nucleic acids were indiscriminately labelled through 10 minutes incubation with Dapi antibody (1:1000, Invitrogen). A final series of 3 minutes rinses in PBS, slides were mounted with coverslips in Immu-mount (Thermo Scientific Shandon) mounting media.

3.3.3. *Microscopic analysis*

3.3.3.A. *Identification of lesion sites*

The result of the immunofluorescent labelling of astrocytes and neurons in brain sections from the animals injected with AA and respective controls was analysed by means of an epifluorescence microscope (BX61, Olympus) coupled with a digital camera system (DP70, Olympus). The lesion sites were identified through the GFAP immunofluorescence detection and using the Cell[^]P imaging software (Olympus) to capture pictures. The lesion site was easily detected in the brains of animals injected with L-Aminoadipate (L- α -AA) by an halo in the tissue without GFAP staining in the medial prefrontal cortex - fig. 4.2A. In the brain sections from control animals, the site of cannula guide placement was confirmed by the physical signs of cannula entry in the brain surface - fig. 4.2 A a1. The site of injection was calculated 1 mm below those marks, as the double internal cannulas projected 1 mm from the cannula guides.

Maps of injection site that indicated the lesion localisation were created - fig 4.1. The animals where the lesion was located outside the medial prefrontal cortex (mPFC) were excluded from the analysis.

3.3.3.B. *Stereological analysis of the affected region*

To further characterise the lesion caused by the L- α -AA injection in the mPFC, we analysed specifically the Cg1, PrL and IL sub-regions, namely by counting the GFAP- and NeuN-positive cells to generally estimate the affection of astrocytes and neurons, respectively. In order to count the cells, 5 μ m spaced z-scan images from the representative brain sections selected previously (see section 3.3.3.A) were obtained using a confocal microscope (Olympus FV1000, Japan) under a 20X objective. Laser excitation wavelengths were set at 405 nm for Dapi, 488 for NeuN and 559 for GFAP secondary antibodies; the pinhole was adjusted to 80.0 μ m. Each of the mPFC subregions were outlined according to the rat brain atlas of Paxinos and Watson [104]. GFAP-positive astrocytes and NeuN-positive neurons were counted using ImageJ (<http://rsbweb.nih.gov/ij/>) with the "Cell counter" plugin in the confocal z-stacks projections, obtained in the Simple Confocal Viewer software v1.0.1. Because the astrocytic morphology may be confusing due to complex processes tree that may overlap with vicinal astrocytes, and fluorescent artefacts may lead to false positives, only co-localisations with DAPI were considered for counting in both cell types. In order to avoid small fluctuations of fluorescent staining quality from slice to slice, the number of cells

counted in the Cg1 and PrL was normalised to the number of cells counted in the IL, a vicinal region spared from the surgical procedure and gliotoxin lesion, resulting in a ratio that allows comparison between different animals.

3.3.4. *Statistical Analysis*

Data are expressed through the study as means \pm SEM. Statistical analysis was performed using the GraphPad Prism 5 software (GraphPad Software, Inc.) for Mac OS X. For the analysis of one variable between two groups of animals, Student's *t-test* (comparing distance travelled, velocity and number of rearings in the OF; the alternation score and the total number of arm entrances in the continuous spontaneous alternation between wt and dnSNARE mice), or Mann-Whitney's test (comparing the indexes of learning and reversal of CON and AA animals in the ASST) were used. Two-way ANOVA analysis and Bonferroni *post-hoc* tests were applied to compare the GFAP/IL or NeuN/IL cells ration in lesioned and non-lesioned sites of brain areas from animals that performed ASST and water maze tests; to compare the performance of AA and CON animals along the stages of ASST; to study the effect of gender and genotype in distance travelled, velocity and number of rearings in the OF and the alternation score and the total number of arm entrances in the continuous spontaneous alternation between wt and dnSNARE mice. For the more complex analysis such as studying the group effect in the water maze performance of rats along the trials (WMT) and rats and mice along the days (RMT), as well as to study the effect of the genotype alone or the genotype and gender in the EPM performance (time spent on, entries and explorations on open and closed arms) and time spent by mice in the center of the OF arena, two-way repeated measures ANOVA and Bonferroni *post-hoc* tests were used. At last, for studying the performance of rats and mice in the reversal learning and probe tasks of the water maze tests, we used multivariate ANOVA (MANOVA) and Bonferroni *post-hoc* tests. The appropriate statistical test is denoted for each experiment in the Results section (see chapter 4). The statistical significance of the comparisons for each statistical test was set with a confidence interval of 95% ($\alpha=0.05$).

4. RESULTS

4.1. Amino adipate pharmacological rat model

4.1.1. Selection of animals and lesion features

Following the microscopy analysis of the brain sections from animals injected with L- α -AA or aCSF, we performed the selection of the animals whose site of injection was within the mPFC- fig. 4.1. From the set of animals that performed the ASST, 7 CON and 6 AA animals were considered for the analysis of the behaviour output, while 6 CON animals and 8 AA animals were considered for the analysis of the behaviour output from the animals that performed water maze tests. In these animals, the centre of the lesion was localised between the medial and dorsal portions of the PrL and Cg1 sub-regions of the medial PFC.

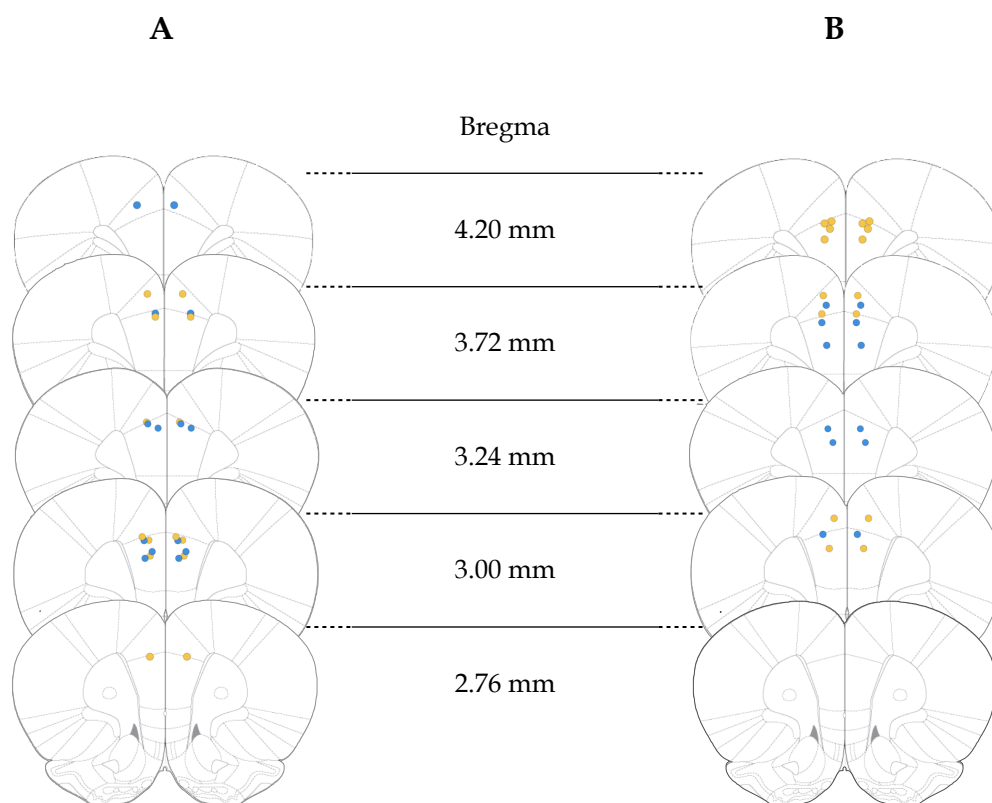


Figure 4.1. Representation of the sites of brain injections, 4.20 mm to 2.76 mm from Bregma. A - Set of animals that performed ASST; B- Set of animals that performed water maze tests, according to the Paxinos and Watson rat brain atlas figures [104]. ● CON; ● AA.

The microscopy analysis of the rats brain tissue preparations revealed that the bilateral injection of L- α -AA induced astrocyte depletion in the whole range of injection, forming an halo within the GFAP staining. Despite of the complete absence of astrocytes, neurons were still detectable within the lesioned area - fig 4.2. The ratio of the GFAP positive cells number of cells in lesion sites over the the number of cells in non-lesioned sites, at the IL and ventral portion of the PrL, illustrates the complete absence of astrocytes in gliotoxin injected subjects. (lesion sites, ASST: CON, n=5 and AA, n=5; water maze tests: CON, n=5 and AA, n=5; non-lesion sites, ASST: CON, n=5 and AA, n=4; water maze tests: CON, n=5 and AA, n=6). Two way ANOVA test pointed out significant differences between the ratio of GFAP positive cells in CON and AA subjects, either in animals that performed ASST, at 3 days post-injection, or water maze tests, at 7 days post injection (ASST, CON: $1. \pm 0.0$, AA, 0.0 ± 0.0 , $t=12.5$, $p<0.001$ - fig 4.2 b1; water maze tests, CON: 1.2 ± 0.1 , AA, 0.0 ± 0.0 , $t=6.7$, $p<0.001$ - fig 4.2 c1). Regarding the non lesioned regions the of GFAP positive cells ratios did not differ between CON and AA animals of the ASST and water maze tests sets (ASST, CON: 1.5 ± 0.1 , AA, 1.4 ± 0.0 , $t=0.7$, $p>0.05$ - fig. 4.2 b2; water maze tests, CON: 1.4 ± 0.1 , AA, 1.4 ± 0.1 , $t=0.2$, $p>0.05$ - fig 4.2 c2). Opposite to what happened with the GFAP immunoreactivity, NeuN stained cells were not affected by the L- α -AA injections, as the two-way ANOVA have not evidenced any differences between groups in lesioned sites either in ASST or water maze tests set of animals (ASST, CON: 1.0 ± 0.1 , AA, 1.1 ± 0.1 , $t=0.4$, $p>0.05$ - fig 4.2 b1; water maze tests, CON: 1.1 ± 0.1 , AA, 0.9 ± 0.2 , $t=1.2$, $p>0.05$ - fig 4.2 c1) And as expected, the same was true in non lesioned sites (ASST, CON: 1.2 ± 0.4 , AA, 1.5 ± 0.1 , $t=0.3$, $p>0.05$ -fig 4.2 b2; water maze tests, CON: 1.6 ± 0.2 , AA, 1.4 ± 0.1 , $t=1.2$, $p>0.05$ - fig 4.2 c2).

4.1.2. Behaviour performance

In order to assess the translation of astrocyte depletion in the behaviour output of the prefrontal cortex, animals injected with the gliotoxin L- α -AA and their respective controls were tested through the ASST and the water maze based tests.

4.1.2.A. Attentional set-shifting task

The ASST allowed assessing the PFC-dependent functions such as attention, dimensional set-shifting and reversal learning [98]. A two-way analysis of variance (two-way ANOVA) of the number of trials to criterion (TC) - number of trials needed by each group of animals (CON, n=7; AA, n= 6) until acquisition of the rule in each stage - showed that animals with

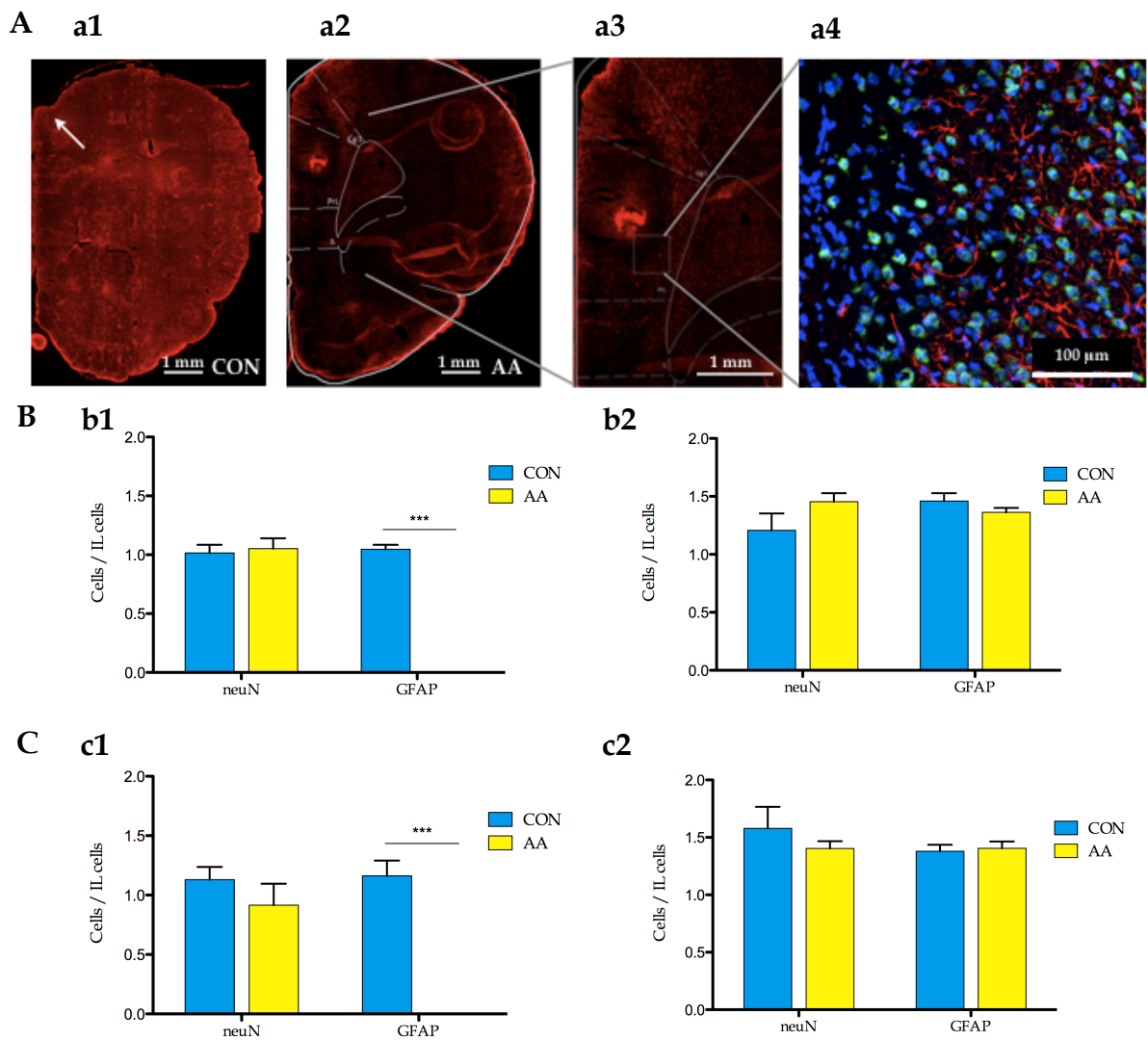


Figure 4.2. Effects of the gliotoxin L- α -AA. **A** - intracranial L- α -AA injections cause astrocytic ablation denoted by an halo of no GFAP immunoreactivity; **a1**- brain section from CON animal; white arrow denotes the physical damage caused by the cannula placement; **a2** - brain section from AA animal evidencing astrocytic ablation in Cg and PrL, detailed in **a3**; **a4** - confocal imaging evidencing no astrocytes within the lesioned area, while neurons were not affected. **B** and **C**- Ratio of the number of cells within lesion sites (Cg1 and ventral portion of PrL) - **b1** and **c1**- over the number of cells in non-lesion region (IL) compared to a non-lesioned region - **b2** and **c2**- in animals that performed ASST, **B** and in animals that performed water maze tests, **C**. *** $p < 0.001$.

astrocyte depletion in the mPFC (AA) have more difficulty to learn to discriminate stimuli in the dimension of textures (SDT: CON 11.7 ± 2.5 TC and AA 31.8 ± 9.3 TC, $t = 2.7$, $p < 0.05$) and to perform reversal learning (Rev1: CON 13.4 ± 2.1 TC and AA 33.5 ± 7.6 TC, $t = 3.0$, $p < 0.05$; Rev2: CON 13.3 ± 2.7 TC and AA 41.0 ± 9.9 TC, $t = 3.8$, $p < 0.01$), when compared to controls (CON) - fig. 4.3. No differences between groups were observed in the remaining stages (SDO: CON 14.6 ± 3.3 TC and AA 20.5 ± 7.5 TC, $t = 1.1$, $p > 0.05$; CDO: CON 15.3 ± 3.3 trials and AA: 13.3 ± 2.2 TC, $t = 0.2$, $p > 0.05$; EDST: CON 16.4 ± 3.9 TC and AA 11.3 ± 2.0 TC, $t = 0.70$, $p > 0.05$).

The index of learning, mean TC from the learning stages (fig. 4.4 A) shows that both groups of animals learn similarly how to discriminate new stimuli along the stages of this task (CON: 14.5 ± 1.6 TC and AA: 19.8 ± 3.2 TC, Mann-Whitney $U= 279.5$, $p>0.05$). However, the index of reversal, mean TC from the reversal stages, points out a striking difference between controls and animals depleted of astrocytes in the mPFC - fig 4.4 B (CON: 13.4 ± 1.7 TC; AA 37.3 ± 6.1 TC, Mann-Whitney $U= 11.5$, $p<0.001$) which confirms the performance observed in both reversal learning stages (fig. 4.3).

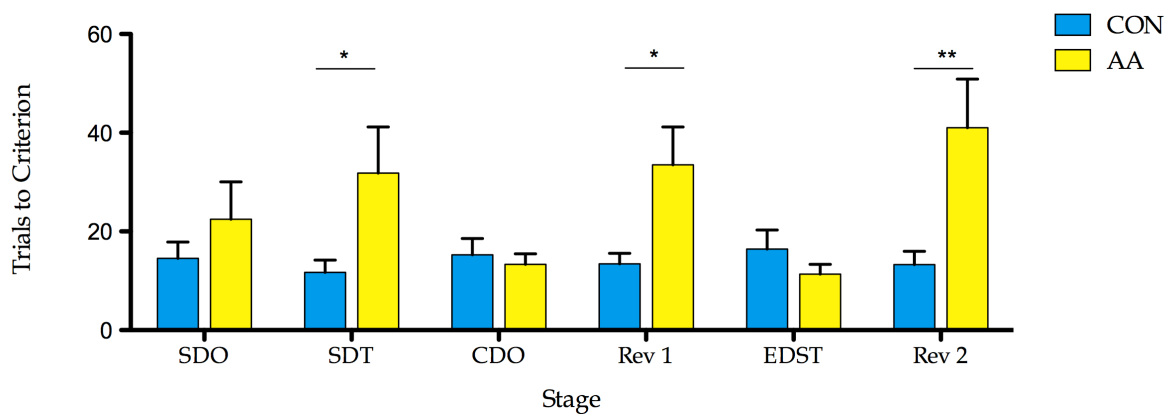


Figure 4.3. Trials to criterion along ASST stages. Rats injected with aCSF (CON) and L- α -AA (AA) Data plotted as mean \pm SEM. * $p<0.05$, ** $p<0.01$.

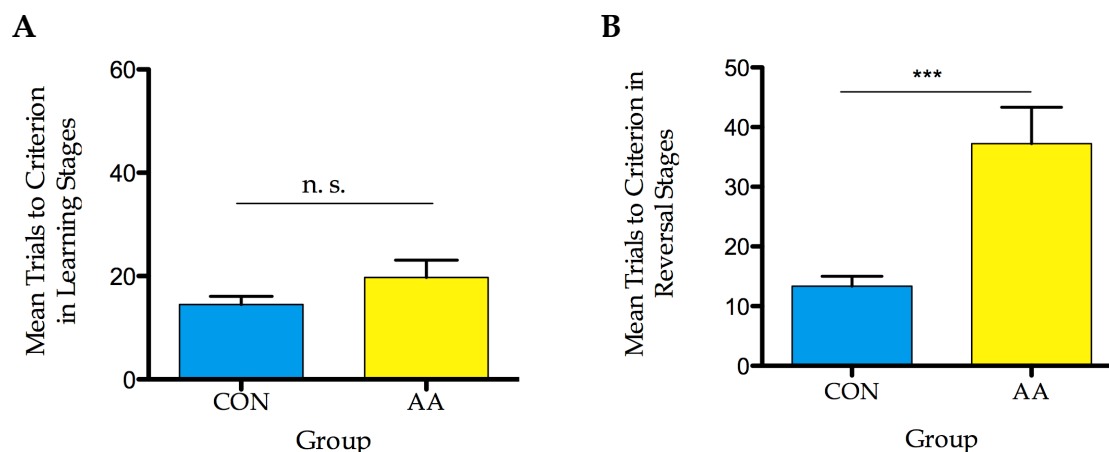


Figure 4.4. Indexes of Learning and Reversal. A - mean trials to criterion in learning stages, Index of learning; and B- mean trials to criterion in reversal stages, index of reversal, of rats injected with aCSF (CON) and L- α -AA (AA). Data plotted as mean \pm SEM. n. s. $p>0.05$. *** $p<0.001$.

4.1.2.B. Water maze based tests

The water maze-based tests allowed assessing spatial working memory (WMT), spatial reference memory (RMT) and reversal learning (RLT) [119] in the animals depleted of astrocytes and respective controls (CON, n=6; AA, n= 8). The analysis of the WMT learning curve (fig. 4.5 A) showed that astrocyte depletion impaired consistently the acquisition process (AA, trial 4: 45.2 ± 7.8 s , $t=2.6$, $p<0.05$) when compared to control animals which showed a typical learning curve along trials (CON, trial 4: 15.3 ± 4.1 s ; $p<0.05$) [119]. In the spatial RMT (fig. 4.5 B) no differences were observed between both groups of animals regarding the shape of the learning curves (day 4: CON 16.4 ± 4.4 s and AA 25.5 ± 5.8 s, $t=1.0$ $p>0.05$). It is noteworthy that in the first day of the task, a difference was observed between both groups (day 1, CON: 40.4 ± 4.1 s, and AA 65.0 ± 6.8 s, $t=2.8$, $p<0.05$), which is a reflex of their different performance in the WMT. In the RLT (fig. 4.6 A) the multivariate ANOVA test evidenced no differences in the percentage (%) of time spent by CON and AA animals in each quadrant. The absence of statistically significant differences in probe test confirms that although a tendency for both groups to spend more time in the quadrant where the platform was located in the RLT (Q4) is observed, both groups of animals failed to learn the RLT since in the probe trial the % time spent in the new quadrant (Q2) does not significantly differ from the % time spent in the old quadrant (Q4) (Q2: CON 32.8 ± 2.8 % and AA 34.1 ± 3.9 %; Q4: CON 27.6 ± 3.5 % and AA 22.5 ± 3.3 %) and does not differ between groups (Q2: CON 32.8 ± 2.8 % and AA 34.1 ± 3.9 %, $t=0.2$, $p>0.05$ - fig. 4.6 B)

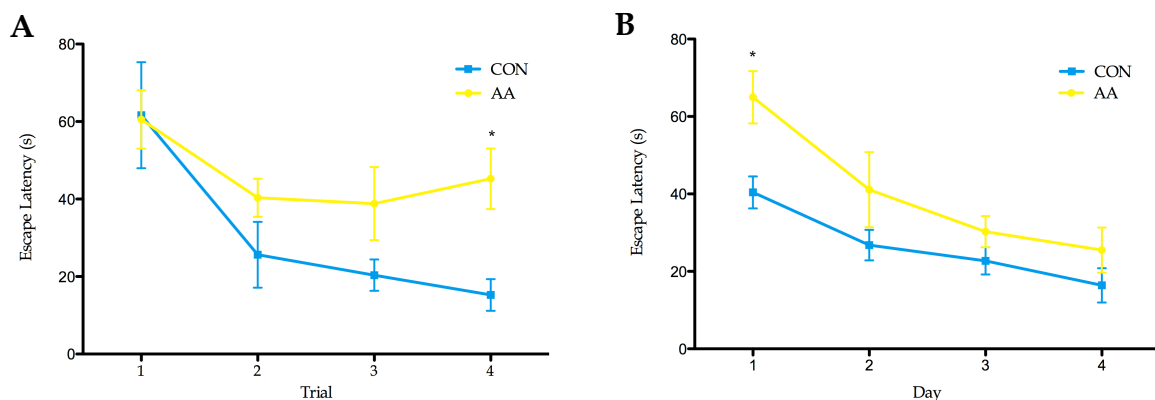


Figure 4.5. Escape latencies (s) in water maze tests. A - Escape latencies (s) in the working memory task, WMT; B -Escape latencies (s) in the spatial reference memory task, RMT of rats injected with aCSF (CON) and L- α -AA (AA). Data plotted as mean \pm SEM. * $p<0.05$.

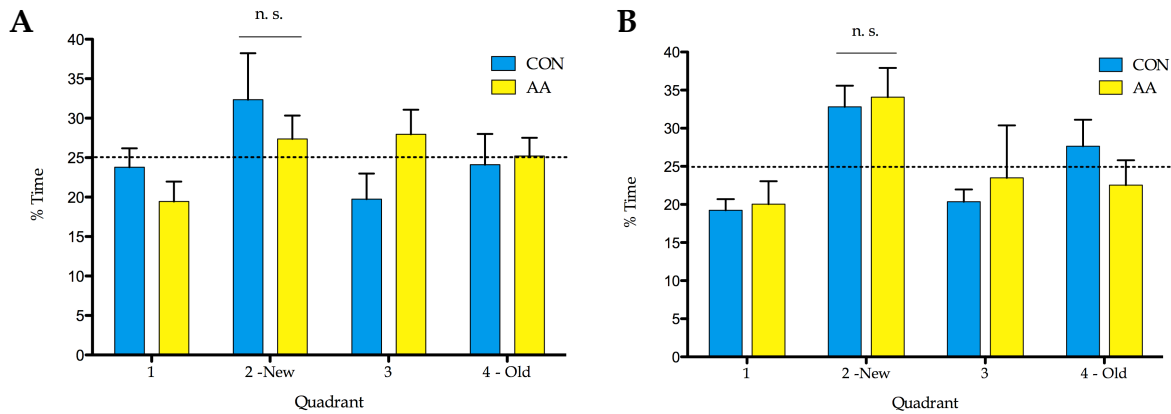


Figure 4.6. Performance of the rats in the reversal learning task, RLT and probe task of the water maze tests. A - Percentage of time (%) spent by rats injected with aCSF (CON) and L- α -AA (AA) in each of the quadrants in the reversal learning task, RLT ; and **B** - in the the probe task. Dotted line represents performance at chance level (25%). Data plotted as mean \pm SEM. n. s. $p > 0.05$.

4.2. *dnSNARE mice model of impaired vesicular release in astrocytes*

After implementation of the dnSNARE colony at the ICVS, 48 animals were generated from crossings between heterozygous GFAP:tTA and tetO.dnSNARE mice. In order to avoid experimental bias, all animals were blind tested as the genotyping was only performed after the behavioural phenotype assessment.

4.2.1. *Genotyping and selection of animals*

The results from the genotyping are summarised in the figure 4.7 A and B. From the 48 animals used in the behavioural phenotype assessment 18 were wt (10 female, ♀ and 8 male, ♂), 8 were dnSNARE (5 ♀ and 3 ♂), 15 were tetO.dnSNARE (5 ♀, and 10 ♂) and 7 were GFAP:tTA (4 ♀ and 3 ♂). Only wild type (wt) animals and double mutant animals (dnSNARE) were considered for the analysis of the behavioural performance in the different tests.

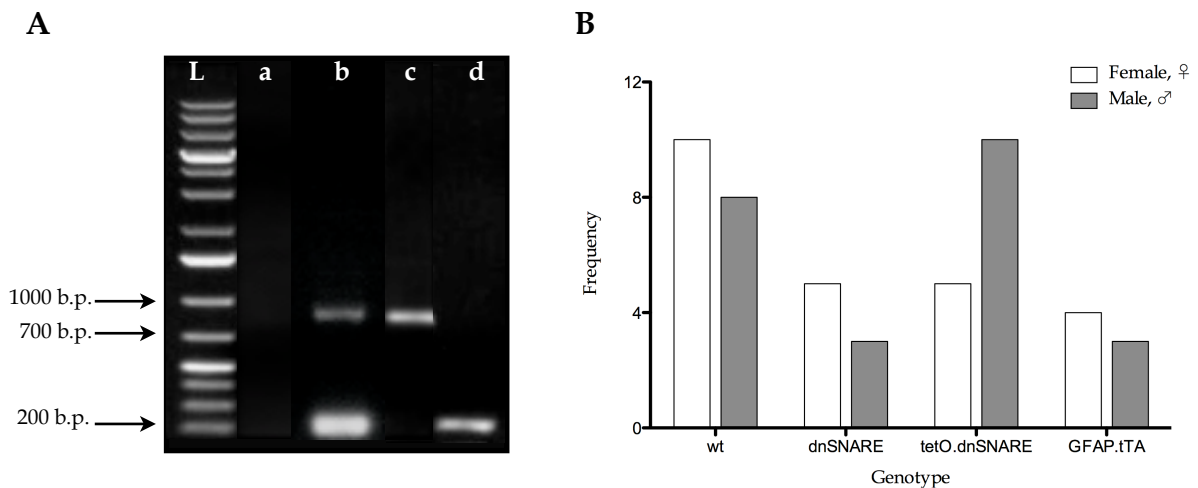


Figure 4.7. Mice genotyping. A- Agarose gel (1% in TAE buffer) with the PCR products of the 4 possible band patterns in for the mice genotyping results. L: ladder (#SM1331, Fermentas); a: wt (C57/Bl6); b: double positive, dnSNARE; c: tetO.dnSNARE ; d: wt (C57/Bl6); d; B- Frequency distribution of the genotypes from the animals generated in the mattings between mice lines GFAP:tTA and tetO.dnSNARE used for the behaviour testing.

4.2.2. Behaviour performance

In order to characterise the behavioural phenotype of the dnSNARE mice strain, 48 animals originated by the matings between the mice lines GFAP:tTA and tetO.dnSNARE were subjected to four behaviour tests: EPM, OF tests, water maze based tests and continuous spontaneous alternation task. These tests aimed to assess anxiety, locomotion and exploratory behaviour, and cognition (memory and learning) of the dnSNARE animals, comparing to their wt littermates.

4.2.2.A. *Elevated plus maze (EPM)*

The elevated plus maze test was used to assess if dnSNARE mice exhibited or not an anxious phenotype [113].

Regarding mice preference for open or closed arms, given by the percentage of time spent in each EPM arms, a two-way repeated measures ANOVA test revealed no significant differences between groups, whether female and male mice where considered together (fig. 4.8 A) in the analysis or not (fig. 4.8 B). In the second analysis, although there were no significant different between groups, dnSNARE male mice tend to spent less time in closed arms (wt ♀: 52.9 ± 3.1 ; wt ♂: 55.6 ± 4.1 ; dnSNARE ♀: 51.4 ± 6.4 ; dnSNARE ♂: 47.8 ± 1.8) that apparently is compensated by the time spent in area that links the two opposite arms of

the plus maze - hub (wt ♀: 13.7 ± 1.9 ; wt ♂: 13.8 ± 1.10 ; dnSNARE ♀: 13.2 ± 2.4 ; dnSNARE ♂: 20.7 ± 2.1).

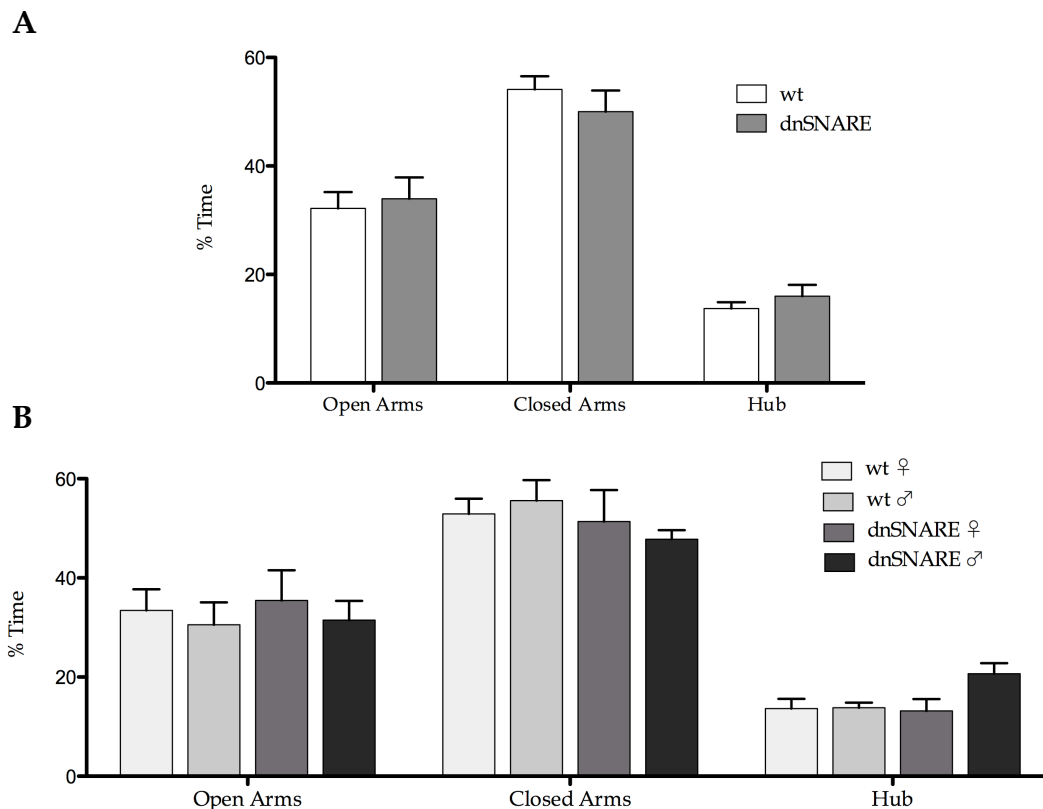


Figure 4.8. Time spent (as percentage of total, %) in the arms and hub of the EPM. A - wt and dnSNARE mice, females and males plotted together; and B - wt and dnSNARE mice, females and males plotted separately. Data plotted as mean \pm SEM.

The number of entrances in open or closed arms did not significantly differ between the groups, either considering both gender together (open arms, wt: 9.0 ± 0.9 ; dnSNARE: 9.9 ± 1.2 ; closed arms, wt: 10.1 ± 1.0 ; dnSNARE: 11.1 ± 1.4 - fig. 4.9 A) or separately (open arms, wt ♀: 8.6 ± 1.1 ; wt ♂: 9.5 ± 1.4 ; dnSNARE ♀: 10.6 ± 1.7 ; dnSNARE ♂: 8.7 ± 1.5 ; closed arms, wt ♀: 9.5 ± 1.5 ; wt ♂: 10.9 ± 1.3 ; dnSNARE ♀: 10.2 ± 1.9 ; dnSNARE ♂: 12.7 ± 1.9 - fig. 4.9 B). The same result was observed in what concerns to the number of arm explorations of female and male together (open arms, wt: 14.5 ± 1.0 ; dnSNARE: 17.1 ± 1.9 ; closed arms, wt: 13.3 ± 1.1 ; dnSNARE: 15.4 ± 2.3 - fig. 4.10 A) and separately (open arms, wt ♀: 14.5 ± 1.6 ; wt ♂: 14.5 ± 1.4 ; dnSNARE ♀: 14.8 ± 2.4 ; dnSNARE ♂: 21.0 ± 1.5 ; closed arms, wt ♀: 12.9 ± 1.4 ; wt ♂: 13.8 ± 1.8 ; dnSNARE ♀: 13.0 ± 2.5 ; dnSNARE ♂: 19.3 ± 4.1 - fig. 4.10 B), indicating the preservation of the exploratory and locomotor activity within all groups of animals. Nevertheless, male dnSNARE mice tended to explore more both open and closed arms.

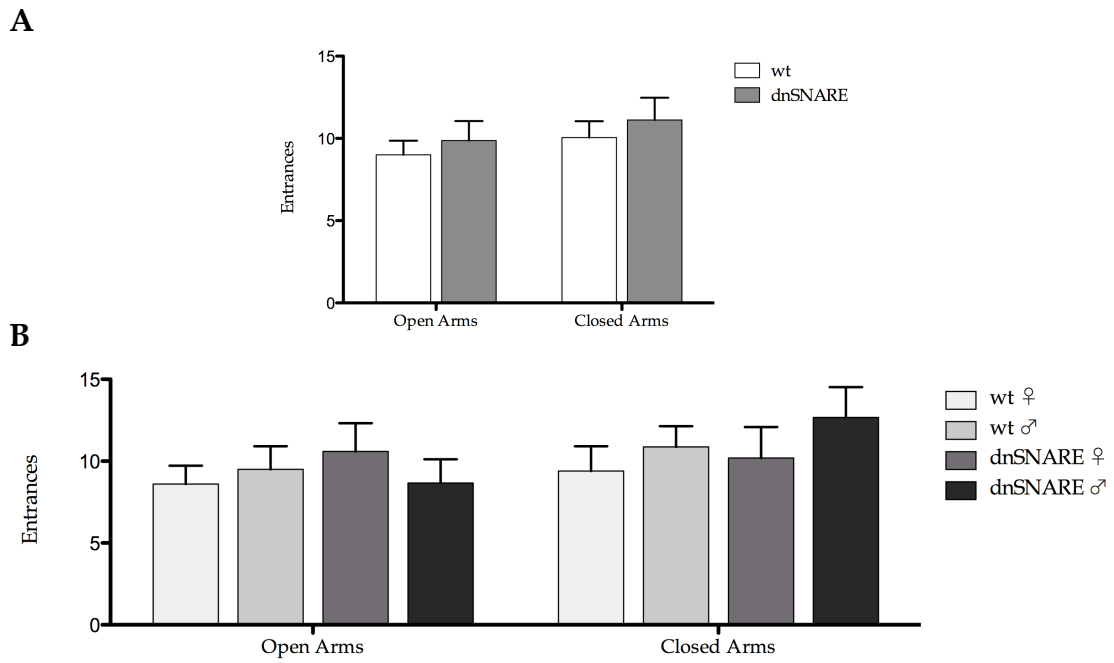


Figure 4.9. Number of entrances in open arms and closed arms of the EPM. A - wt and dnSNARE mice, females and males plotted together; and B - wt and dnSNARE mice, females and males plotted separately. Data plotted as mean \pm SEM.

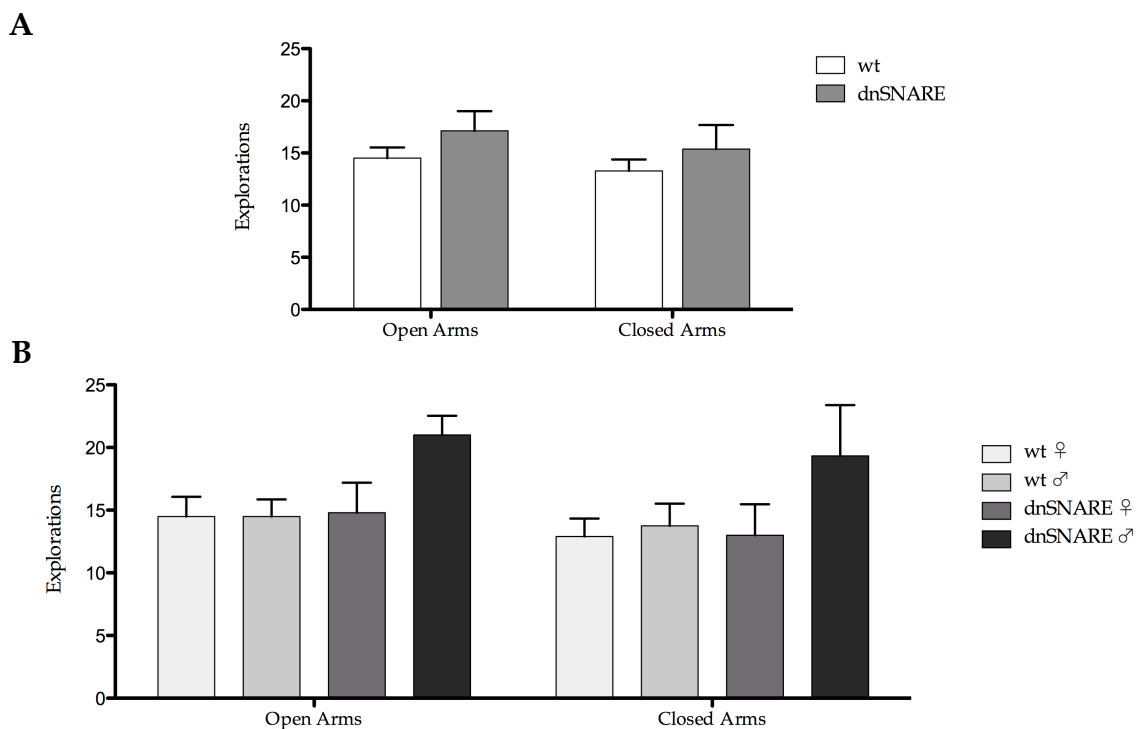


Figure 4.10. Number of explorations in open arms and closed arms of the EPM. A - wt and dnSNARE mice, females and males plotted together; and B - wt and dnSNARE mice, females and males plotted separately (B). Data plotted as mean \pm SEM.

4.2.2.B. Open Field test (OF)

The spontaneous locomotor activity, exploratory behaviour and also possible anxiogenic-like behaviour (tendency to spend more time in the periphery, close to the walls - thigmotaxis) of dnSNARE mice were further analysed in a OF arena [116].

In what concerns to the locomotor activity, no significant differences were found in the distance travelled (fig. 4.11 A and B) and velocity between wt or dnSNARE mice (fig. 4.12 A and B), considering both genders together or separately. In the first parameter, t-test showed no significant differences between the groups (wt: 2906.0 ± 194.0 cm, dnSNARE: 2907.0 ± 291 cm; $t=0.0$, $p>0.05$) and a two-way ANOVA revealed no differences in the distance travelled within mice of the same genotype but different sex (wt ♀: 2824.3 ± 315.8 cm, wt ♂: 2977.7 ± 254.4 cm, dnSNARE ♀: 2833.4 ± 274.3 cm, dnSNARE ♂: 3005.9 ± 658.9 cm). In the velocity, no differences were evidenced by the t-test considering the two genotypes (wt: 9.1 ± 0.78 cm/s, dnSNARE: 8.9 ± 0.7 cm/s, $t=0.6$, $p>0.05$), and by the two-way ANOVA, taking into account both genotype and sex (wt ♀: 9.6 ± 1.3 cm/s; wt ♂: 8.5 ± 0.9 cm/s ; dnSNARE ♀: 7.6 ± 1.0 cm/s; dnSNARE ♂: 9.3 ± 0.6 cm).

The exploratory behaviour, given by the number of rearings that mice do during the 5 minutes of testing in the OF, was similar between both genotypes - fig. 4.13 A (wt: 50.1 ± 5.2 and dnSNARE: 60.3 ± 3.3 , $t=1.3$, $p>0.05$) and gender within each genotype - fig 4.13 B (wt ♀: 43.3 ± 4.2 , wt ♂: 56.1 ± 8.7 , $t=1.3$, $p>0.05$; dnSNARE ♀: 59.7 ± 5.8 , dnSNARE ♂: 61.0 ± 3.1 , $t=0.1$, $p>0.05$).

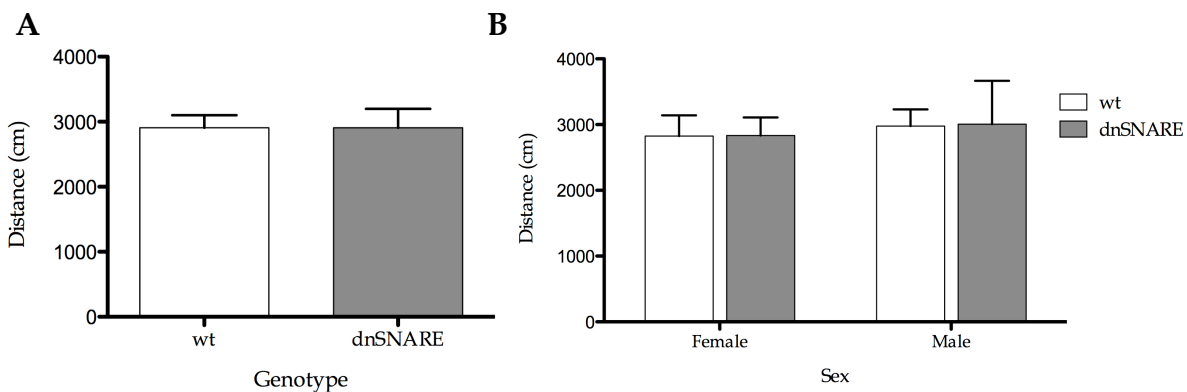


Figure 4.11. Distance travelled (cm) in the open field arena. A - wt and dnSNARE mice, females and males plotted together; and B - wt and dnSNARE mice, females and males plotted separately. Data plotted as mean \pm SEM.

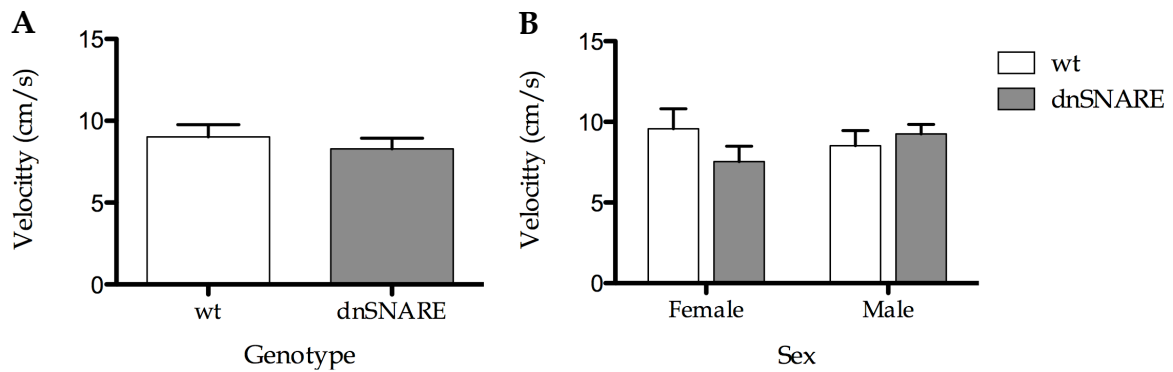


Figure 4.12. Velocity (cm/s) in the open field arena. A - wt and dnSNARE mice, females and males plotted together; B - wt and dnSNARE mice, females and males plotted separately. Data plotted as mean \pm SEM.

The last parameter analysed in the OF test, time spent on centre, was also similar in dnSNARE mice and their wt littermate controls. Comparing the two genotypes including females and males, t-test showed no significant differences (wt: 21.6 ± 4.1 , dnSNARE: 17.7 ± 2.2 , $t=0.63$, $p>0.05$ - fig. 4.14 A) as well as no significant effect of gender was evidenced in either wt or dnSNARE mice, by the two-way ANOVA (wt ♀: 18.0 ± 4.5 , wt ♂: 24.8 ± 6.7 ; $t=0.1$, $p>0.05$; dnSNARE ♀: 17.0 ± 3.8 , dnSNARE ♂: 18.6 ± 1.9 , $t=0.7$, $p>0.05$ - fig. 4.14 B). This means that wt and dnSNARE mice, either female or male, have similar thigmotaxic behaviour when subjected to the OF test.

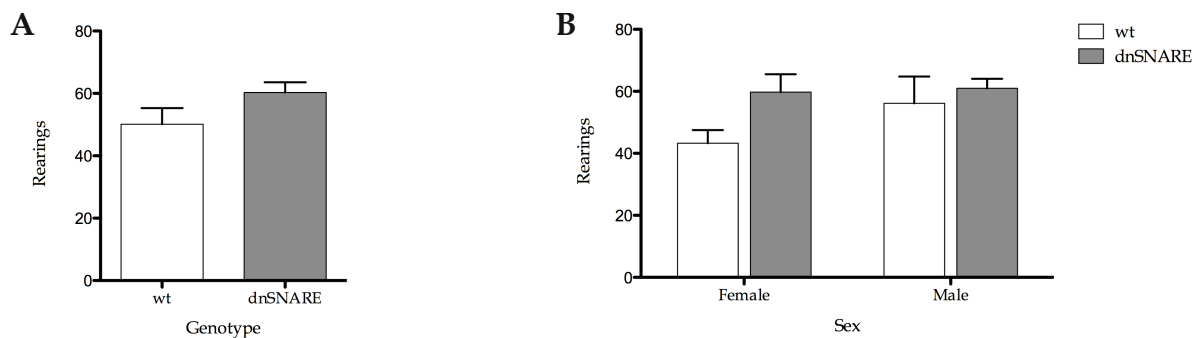


Figure 4.13. Number of rearings in the open field arena. A - wt and dnSNARE mice, females and males plotted together; and B - wt and dnSNARE mice, females and males plotted separately. Data plotted as mean \pm SEM.

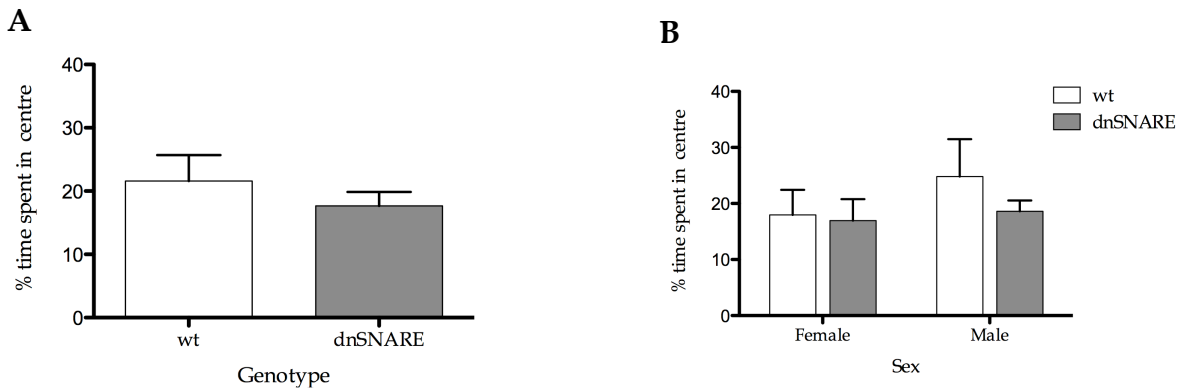


Figure 4.14. Time (as percentage of total, %) spent in the center of the open field arena. A - wt and dnSNARE mice, females and males plotted together; and B - wt and dnSNARE mice, females and males plotted separately. Data plotted as mean \pm SEM.

4.2.2.C. Water maze based tests

Following the characterisation of the locomotor activity, exploratory and anxiogenic behaviour, mice performed cognitive tests to assess their learning and memory abilities, and check whether astrocytic vesicular release is important for these tasks. The first cognitive tests performed were the water maze based tests, that aim to evaluate the spatial reference memory and the reversal learning of dnSNARE animals in comparison to their littermate wt controls.

The spatial reference memory task of the water maze revealed spatial memory impairment of the dnSNARE mice, since in the last day of the task they needed significantly more time to find the submerged platform than wt animals, when analysing female and male animals together (day 4, wt: 29.4 ± 4.9 s, dnSNARE 66.5 ± 12.1 , $t=3.4$, $p<0.01$ - fig 4.15 A). However, this impairment is no longer evident if female and male animals were considered separately within the two genotypes (day 4, wt ♀: 32.3 ± 7.9 s, wt ♂: 25.9 ± 5.5 s, dnSNARE ♀: 62.4 ± 15.4 s, dnSNARE ♂: 73.5 ± 23.1 s - fig. 4.15 B).

In the reversal learning task mice were required to find the platform in the quadrant of opposite location (Q2) relative to the one in the spatial reference memory task (Q4). The ability of learning a new location of the platform was assessed in terms of the mean percentage of time spent in each of the imaginary quadrants along the 3 trials of the task. The more time spent in the Q2, the more capable mice were to find the platform in its new location. Through the MANOVA test and Bonferroni *post-hoc* tests significant differences were found, within groups, in the time spent in each of the imaginary quadrants, by wt mice

(Q1: 25.8 ± 1.4 %, Q2: 32.2 ± 1.9 %, $t=2.4$, $p<0.05$; Q2: 32.2 ± 1.9 %, Q3: 21.7 ± 1.5 %, $t= 3.9$, $p<0.001$; Q2: 32.2 ± 1.9 %, Q4: 20.2 ± 1.9 %, $t= 4.5$, $p<0.001$) and dnSNARE mice (Q2: 32.4 ± 3.1 %, Q4: 19.2 ± 1.6 %, $t= 3.3$, $p<0.01$) - fig. 4.16 A. However, no significant differences were found in the time spent in each quadrants between groups of mice. Furthermore, taking into account both genotype and gender of animals in each group (fig. 4.16 B), significant differences were found within animals of the same group and sex regarding the time spent in the quadrant of the new location of the platform (Q2), when compared to the time spent in other quadrants (wt ♀: Q2, 30.4 ± 2.5 %, Q4, 21.0 ± 2.6 %, $t= 2.7$, $p<0.05$; wt ♂: Q2, 34.4 ± 2.7 %, Q3, 19.7 ± 1.3 %, $t=3.8$, $p<0.01$; Q2, 34.4 ± 2.7 %, Q4, 19.2 ± 2.8 %, $t= 3.9$, $p<0.001$; dnSNARE ♀: Q2, 33.9 ± 4.9 % and Q4, 19.9 ± 2.2 %, $t= 2.8$, $p<0.05$). Overall, it is notorious that mice with astrocytic dysfunction and their littermate controls were able to learn the new location of the platform, indicating an intact reversal learning.

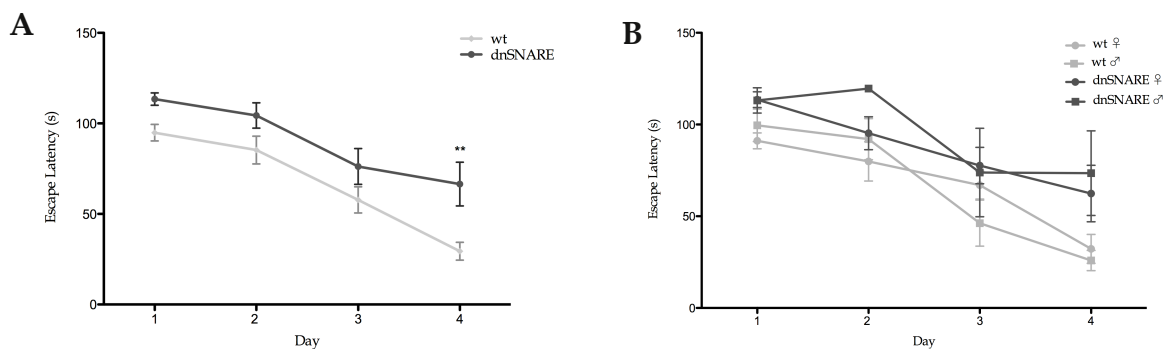


Figure 4.15. Escape latency (s) in the spatial reference memory task, RMT. A - Escape latency by genotype, with both gender plotted together; and **B -** Escape latency by genotype, with both gender plotted separately, in mice with astrocytic dysfunction (dnSNARE) and their littermate controls (wt). Data plotted as mean \pm SEM. ** $p<0.01$, compared to wt littermate controls.

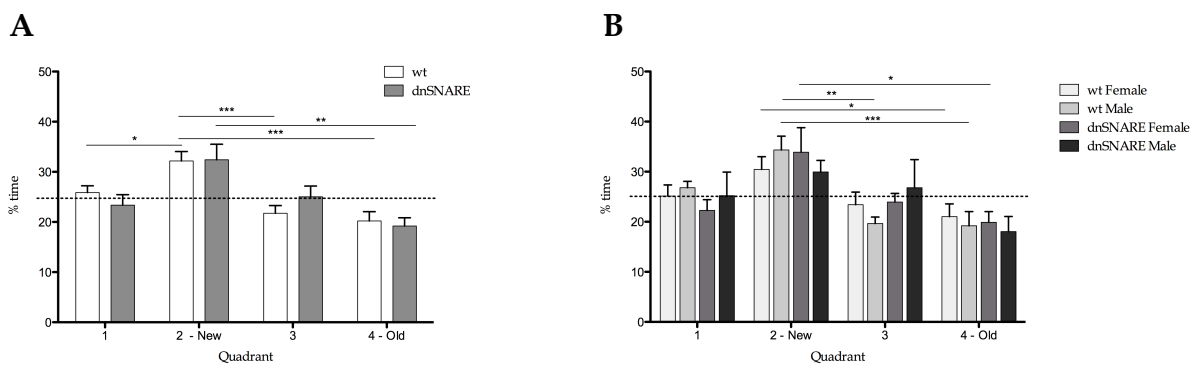


Figure 4.16. Performance in the reversal learning task, RLT. **A** - time (%) spent in each of the imaginary quadrants of the water maze by mice with astrocytic dysfunction (dnSNARE) and their littermate controls (wt), plotted per genotype; and **B** - time (%) spent in each of the imaginary quadrants of the water maze by mice with astrocytic dysfunction (dnSNARE) and their littermate controls (wt), plotted per genotype and sex. Dotted line represents performance at chance level (25%). Data plotted as mean \pm SEM; * $p < 0.05$, ** $p < 0.01$, *** $p < 0.001$.

4.2.2.D. Continuous spontaneous alternation test

While the water maze based tests assessed spatial reference memory and reversal learning of wt and dnSNARE animals, the continuous spontaneous alternation test allowed to characterise the spatial working memory of these animals. Making an overall analysis, with no gender discrimination, to the percentage of arm alternations (alternation score, %) from the two mice groups, t-test showed no significant differences between wt and dnSNARE mice (wt: 28.0 ± 1.6 %; dnSNARE: 29.2 ± 2.4 %, $t=0.4$, $p > 0.05$) - fig 4.17 A. However, when the animals gender was taken into account for the statistical analysis, significant differences were found between subjects of different genotype and within the same gender - dnSNARE male mice have higher alternation score which means improved working memory, when compared to their littermate wt male controls (wt σ^7 : 26.2 ± 1.6 %, dnSNARE σ^7 : 36.7 ± 3.3 %, $t=2.5$, $p < 0.05$). Regarding female subjects, no differences were found between both genotypes (wt f : 29.0 ± 2.6 %, dnSNARE f : 27.5 ± 1.1 %, $t=0.6$, $p > 0.05$) - fig 4.17 B. As no genotype-effect (wt: 24.3 ± 1.0 %, dnSNARE: 21.5 ± 0.6 %, $t= 1.8$, $p > 0.05$ - fig. 4.18 A) or genotype-by-sex interaction (wt f : 23.2 ± 1.3 %, dnSNARE f : 21.6 ± 0.6 %, $t=0.8$, $p > 0.05$; wt σ^7 : 25.8 ± 1.7 %, dnSNARE σ^7 : 21.3 ± 0.9 %, $t=1.7$, $p > 0.05$ - fig. 4.18 B) were observed regarding the total number of arm entries, the greater alternation score of dnSNARE male mice is attributable to an improved spatial working memory and not to a greater locomotor activity or motivation to explore the maze.

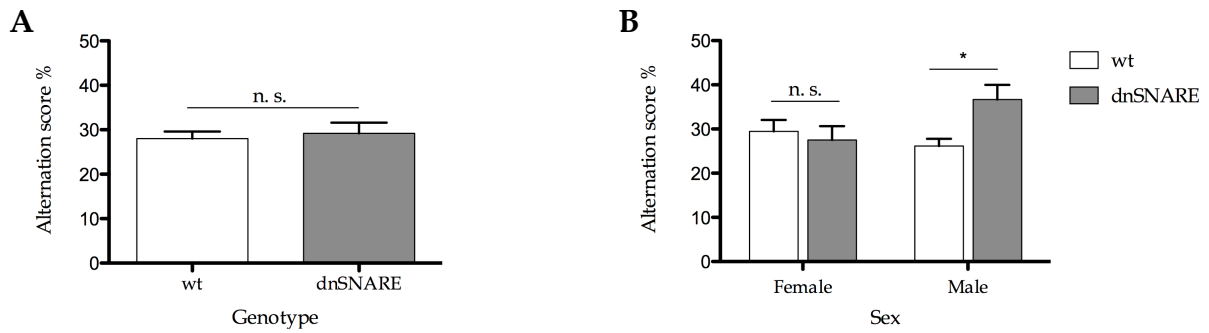


Figure 4.17. Arm alternation (alternation score, %) in the continuous spontaneous alternation task, performed in the Y-maze. A - alternation score of mice with astrocytic dysfunction (dnSNARE) and their littermate controls (wt), plotted per genotype; and **B** - alternation score of mice with astrocytic dysfunction (dnSNARE) and their littermate controls (wt), plotted per genotype and sex. Data plotted as mean \pm SEM. ; n. s. $p > 0.05$, * $p < 0.05$.

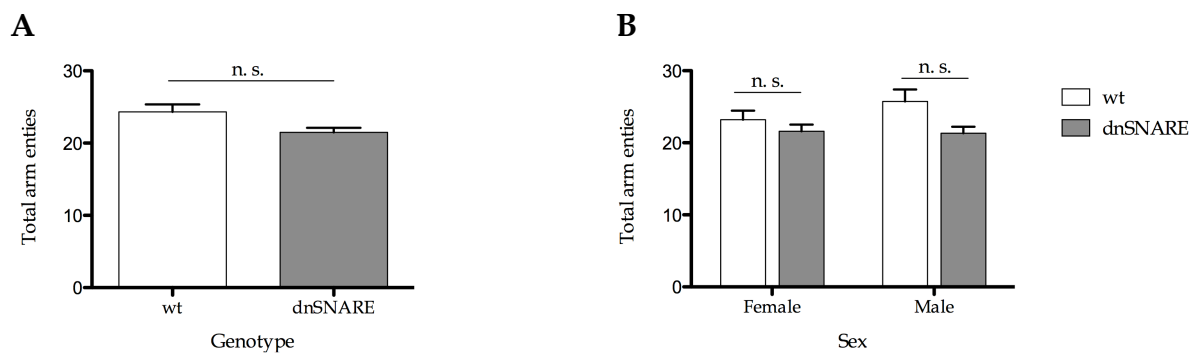


Figure 4.18. Total arm entries in the continuous spontaneous alternation task, performed in the Y-maze. A - total arm entries of mice with astrocytic dysfunction (dnSNARE) and their littermate controls (wt), plotted per genotype; and **B** - total arm entries of mice with astrocytic dysfunction (dnSNARE) and their littermate controls (wt), plotted per genotype and sex. Data plotted as mean \pm SEM. ; n. s. $p > 0.05$.

5. DISCUSSION AND CONCLUSION

The main aim of this work was to implement and study animal models of astrocytic dysfunction and assess if these animals would display cognitive differences when compared to the respective controls, as a way to dissect the astrocytic role in the construction of complex behaviour outputs. Here we show the implementation process and the first results of the behavioural phenotype characterisation of learning and memory, in the two models: one pharmacological rat model, with a single bilateral intracranial injection of L- α -amino adipate in the mPFC that depletes astrocytes in the region; and one genetic mice model, consisting of a conditional blockade of the exocytotic release in astrocytes by means of a “tet-Off” system.

During the establishment of the first model, multiple parameters required careful adjustment: from the surgical procedure for the cannula implementation (the choice of stereotaxic coordinates and the method of fixing the cannula to the skull); recovery period before drug administration; drug administration (concentration, vehicle and infusion rate, and methods for rat restraint during the drug infusion - implicating the establishment of a new anaesthesia protocol); lag phase between drug administration and behavioural testing; to histological analysis (brain sections immunofluorescence) and correlation to the behavioural output of rats with astrocytic ablation. Nevertheless, after all parameters were defined, the experiments carried out with this rat model of pharmacological astrocytic ablation provided us several interesting results.

Before the behavioural output analysis, we started to get an insight into the real location of the cannula and into the extent of the lesion caused by the drug injected through the bilateral internal cannula, as well as the kind of collateral damage due to the cannula implantation itself. By following the established stereotaxic coordinates, we were able to target the medial and dorsal portions of the PrL and the Cg regions of the PFC. The determination of the number of GFAP- and NeuN-positive cells, through confocal imaging, allowed to further characterise the cortical tissue subjected to the injections of L- α -AA or aCSF. The observation of astrocyte depleted areas within the mPFC of animals that performed ASST and water maze based tests evidenced the astrocyte ablation by L- α -AA as a dynamic lesion. Apart from complete absence of GFAP staining in the lesion site of animals injected with L- α -AA, we observed that the lesions in animals that performed water maze tests (sacrificed 7 days post-drug infusion) were relatively smaller than the ones observed in animals that performed ASST (sacrificed 3 days post-drug administration), although due to the method of selection of brain sections we could not quantify the lesion size. This

observation correlates with the dynamic status of the L- α -AA caused astrocyte ablation [89]. Moreover, this fact suggests a repopulation of the lesioned area by other astrocytes whose origin and functional integration into the existing glial network needs to be clarified [120]. Despite of the absence of astrocytes within lesioned areas, the number of neurons was not affected within these areas.

From the behaviour assessment of the rats subjected to the bilateral intracranial injections of L- α -AA we could conclude that the astrocytic ablation in the mPFC affects the attentional set-shifting, the working memory and the reversal learning. First, by performing the ASST, AA animals have shown difficulty to discriminate textures in the SDT stage, but this was not observed in the precedent discrimination of odours because rodents are very sensitive to olfactory stimuli [121]. Apparently, astrocyte depletion impairs the learning of the discrimination of stimuli from a new dimension (texture). In CDO and EDST (corresponding to a compound discrimination of textures), animals injected with the gliotoxin have shown similar performance to the control animals. But the depletion of astrocytes caused a strikingly worse performance in the reversal stages, which indicates an impairment of the reversal learning. These observations are consistent with the fact that the mPFC mediates shifts between new strategies or rules [122]. Nevertheless, these observations do not comply with the data observed in the RLT of the water maze, as the similar performance of AA and CON animals in the reversal learning and probe task of the water maze based tests (7 days post-injection) suggests that were not result of the astrocyte depletion lesions. That could be explained by the fact that astrocyte ablation lesions were considerably smaller in animals that performed water maze based tests, than in animals that performed ASST [89]. Concerning the other tasks of the water maze based tests, astrocyte depleted animals displayed impaired working memory, which is a cognitive function dependent on the regions affected [99]. The learning curve in the RMT was similar in both groups of animals, except for the first day of this task, where differences between groups escape latencies reflect a working memory impairment in AA animals. Indeed, an intact mPFC is necessary for proper working memory, but not for spatial learning and memory [110].

Together, these observations go against the classical concept that learning and memory processes are exclusively result of the neuronal activity and supports the tripartite synapse theory [32], meaning that astrocytes are crucial for such cognitive processes.

In order to identify a possible mechanism for the effects observed in the astrocyte depletion model, we implemented the dnSNARE mice model [106] at our lab, so that we could study the impact of astrocytic vesicular release of neurotransmitters in the build-up of complex behaviour forms. For the establishment of the transgenic mice dnSNARE model in our lab, the GFAP.tTA and tetO.dnSNARE mice lines kindly supplied by the lab of Philip Haydon (Tufts University, Boston) were first maintained in heterozygous state before we

could start with the matings between mice of these two lines. Animals GFAP:tTA and tetO:dnSNARE generated by the back-crossings were then mated to produce dnSNARE mice. This whole process lasted for several months, since we needed a considerable number of animals suitable to perform all behaviour tests (at least 3 animals of each genotype and sex). Once mice from the matings between the two different mice lines reached 10 weeks old they, we had for the first time in our lab mice with exocytotic release blockade in astrocytes ready to behaviour phenotype characterisation. Initially, our main focus was to characterise dnSNARE behavioural performance in cognitive tests that assessed learning and memory, but as this mice line was being established for the first time in our lab, we decided to go further on the behavioural phenotype characterisation. Hence, we opted to test these animals in the EPM, the OF, the water maze tests and the continuous spontaneous alternation test in the Y-maze to screen additionally for cognition, exploratory motivation, locomotion difficulties or anxiety, as this mice strain was only tested by other groups by the the novel object recognition task [40, 90], in the context of sleep deprivation, and in the zero maze, to assess anxiety levels [40].

In the EPM test, mice preference for closed arms was not different from their preference for closed arms, regarding genotype and sex, meaning that wt and dnSNARE animals have the similar anxiety level. However, male dnSNARE mice tended to spend less time in the closed arms, apparently compensated by the time spent in the hub. But since the number of arm entries and explorations was similar in all mice groups, the tend for dnSNARE male mice spend less time in closed arms and to explore more both open and closed arms was not due to different locomotor and exploratory activity. These similarities in the anxiety level of dnSNARE mice and littermate wt controls assessed in the EPM are consistent with the ones already reported in the zero maze by Halassa and colleagues [39]. This means that the fact that the blockade of exocytotic release in astrocytes per se is not sufficient to cause an alteration in the anxiety patterns in these animals.

Open field arena testing revealed no significant differences between wt and dnSNARE mice locomotor activity (distance travelled and velocity), exploratory behaviour (rearings) and thigmotaxis (related to the time spent in the centre of the arena). The thigmotaxis results of wt and dnSNARE mice are coherent with the similar anxiogenic level between these animal observed by us in the EPM. Once again, we can say that the condition of astrocytic dysfunction in terms of vesicular release has no impact in the locomotor activity, exploratory and thigmotaxic behaviour.

Since we achieved the characterisation of locomotor, exploratory and anxious behaviour in mice with astrocytic dysfunction and confirmed that both genotypes were similar in these characteristics (and therefore they would not influence the motivation to perform additional tests) we aimed to further characterise these dnSNARE and wt littermates in what concerns

to their learning and memory abilities. The water maze based tests revealed an impairment of the spatial reference memory of dnSNARE animals when compared to littermate wt controls, with no gender discrimination. However these differences are no longer evident when female and male mice from the two genotypes were considered to the analysis separately. This means that the gender of the animals has no effect in the behavioural output of control and dnSNARE mice and suggests that differences are only evident when the number of animals per group is increased. Following the reference memory task, wt and dnSNARE animals performed the RLT, on which animals from both genotypes have learnt the new location of the platform (Q2). Even so, wt animals seem to be more effective than dnSNARE animals in the learning of the new platform location, as the first spent significantly more time in the Q2 than in any other quadrant, while the time spent by the seconds in the Q2 was only significantly different in comparison to the Q4. Apparently, wt animals are more objective when navigating towards the platform, while the navigation of dnSNARE animals seems more disperse in the four quadrants of the water maze. The analysis of this data separately for females and males from each group evidenced that both female and male wt mice were able to learn the new location of the platform, while within the dnSNARE genotype, only female could learn to reach the platform in the Q2, instead of the Q4.

With the water maze tests we could, assess the reference memory, dependent on the hippocampus and the reversal learning, dependent on the PFC. Since we were interested in further characterise the PFC function of dnSNARE, we opted to also test them through the continuous spontaneous alternation test in a Y-shaped maze. This test allowed us to characterise the terms of spatial working memory of animals with astrocytic dysfunction. When placed in the centre and allowed to explore the maze during 5 minutes, dnSNARE male animals revealed improved working memory, as they got a higher alternation score than wt male mice, even with similar locomotor and exploratory activity, comparing to other groups of animals, of different genotype and sex.

To our knowledge, we are first reporting behavioural phenotype characterisation of dnSNARE mice terms of: anxiety level in the elevated plus maze; locomotor, exploratory and thigmotaxic activity in an OF, spatial reference memory and reversal learning in a water maze and spatial working in a Y-shaped maze. Along all this behavioural phenotype characterisation, we could observe that the gender may have an effect in the behaviour output of the dnSNARE animals. This idea is supported by the results obtained in the reversal learning task of the water maze bases tests and also in the continuous spontaneous alternation test. In either of those, male dnSNARE animals revealed a behaviour phenotype distinct from female subjects: in the reversal learning task of the water maze based tests, female subjects had better performance, while in the continuous spontaneous alternation

task male subjects have performed better. Therefore, the performance of males and females should be considered individually, at least in water maze tests and in the continuous spontaneous alternation test.

Overall, astrocyte depletion in the mPFC induced and impairment of behavioural functions dependent on this region, such as working memory and reversal learning. These findings are in line with the data obtained from the cognitive characterisation of the dnSNARE mice, which display impaired vesicular release by astrocytes and therefore impaired gliotransmission. Altering astrocytic function at this level causes changes in the behaviour output, as these animals showed impairment in the reference learning and curiously an improvement in working memory. It seems that the outputs observed require different mechanisms, which represent new scientific questions in this field. In the case of the gliotoxin astrocytic depletion, it is obvious that all the astrocyte functions in brain metabolism (bridging the nutrient passage from blood to neurons) [24] and homeostasis of ions ($[K^+]$ and $[H^+]$) [16] and neurotransmitters [14, 17-20] are arrested in lesioned sites, compromising the neuronal activity in those region. Besides the classically accepted functions of astrocytes [15], all the astrocytic implications in the modulation of the synaptic transmission [32] and integration of neuron-glia circuits [41] are also interrupted. Therefore, it would be expectable that the cognitive functions of the gliotoxin-injected animals would be somehow compromised. However, as the lesion caused by L- α -AA is so severe, the dissection of the mechanisms underlying the obtained behavioural phenotypes gets complicated. With the assessment of the behavioural phenotype of the dnSNARE mice, the behavioural output of these animals is easily attributed to the blockade of the gliotransmitter release in GFAP-expressing astrocytes, since the formation of SNARE complex for the docking of gliotransmitter-containing vesicles does not occur in these animals [106, 107]. Nevertheless, we cannot point out which of the absent gliotransmitters is making the difference, but we can speculate about it. Could be ATP or glutamate, once these are the most recognised chemical transmitters that mediate astrocyte-neuron signaling [123], or even D-serine, because it has been recently identified as major gliotransmitter in the central nervous system that serves as an endogenous ligand for the glycine site of NMDA receptors [55, 124-127]. However, either glutamate or D-serine seem to have more relevance because the most common forms of synaptic plasticity found in the brain are dependent of the activation of NMDA receptors, including long-term potentiation (LTP) and long-term depression (LTD), which are in the cellular substrates of cognitive learning and memory [128].

We show here interesting results, regarding the influence of astrocytes in complex cognitive functions. However, further studies are required to help the elucidation of the

mechanisms involved such as using electrophysiological and neurochemical techniques to understand how brain dynamics are altered and if those alterations can be correlated with others observed under pathological states.

With the present work we have attained the successful implementation in our lab of two different animal models of astrocytic pathologies. The amino adipate pharmacological rat model, was established through surgery and post-recovery drug infusion, while the transgenic mice model required multiple matings between different mice lines and selection of offspring for the obtention of the dnSNARE animals and their wt littermate controls. Despite the distinct nature of these two animals models, we were able to characterise its behaviour phenotype in the pathological conditions induced, leaving these available for further studies in our lab. From now on, we can use these models to study brain function in conditions of stress or dementia to try to disclose more about astrocytes role.

6. REFERENCES

- 1 Virchow, R. (1856) *Gesammelte Abbildung zur wissenschaftlichen Medizin. Verlag von Meidinger Sohn & Comp*
- 2 Virchow, R. (1858) *Die Cellularpathologie in ihrer Begründung auf physiologische and pathologische Gewebelehre. Zwanzig Vorlesungen gehalten während der Monate Februar, März und April 1858 im pathologischen Institut zu Berlin. August Hirschwald*
- 3 Golgi, C. (1873) *Suella struttura della sostanza grigia del cervello (comunicazione preventiva). Gazzetta Medica Italiana, Lombardia 33, 244-246*
- 4 Golgi, C. (1903) *Opera Omnia.*
- 5 Kettenmann, H. and Verkhratsky, A. (2008) Neuroglia: the 150 years after. *Trends in Neurosciences 31, 653-659*
- 6 Kölliker, A. (1889) *Handbuch der Gewebelehre des Menschen.*
- 7 Andriezen, W.L. (1893) The neuroglia elements of the brain. . *British Medical Journal 2, 227-230*
- 8 Ramón y Cajal, S. (1913) *Sobre un nuevo proceder de impregnacion de la neuroglia y sus resultados en los centros nerviosos del hombre y animales. Trab. Lab. Invest. Biol. Univ. Madrid 11*
- 9 Rio-Hortega, P. (1919) *El tercer elemento de los centros nerviosos. Biol. Soc. Esp. Biol. 9, 69-120*
- 10 Rio-Hortega, P. (1921) *Estudios sobre la neuroglia. La glia de escasas radiaciones oligodendroglia. Biol. Soc. Esp. Biol. 21, 64-92*
- 11 Rio-Hortega, P. (1932) *Microglia. In Cytology and Cellular Pathology of the Nervous System. Penfield, W., ed.*
- 12 Weigert, K. (1895) *Beiträge zur Kenntnis der normalen menschlichen.*
- 13 Bushong, E.A., et al. (2002) *Protoplasmic astrocytes in CA1 stratum radiatum occupy separate anatomical domains. Journal of Neuroscience 22, 183-192*
- 14 Nedergaard, M., et al. (2003) *New roles for astrocytes: redefining the functional architecture of the brain. Trends in Neurosciences 26, 523-530*
- 15 Wang, D.D. and Bordey, A. (2008) *The astrocyte odyssey. Progress in Neurobiology 86, 342-367*
- 16 Kimelberg, H.K. (2007) *Supportive or information-processing functions of the mature protoplasmic astrocyte in the mammalian CNS? A critical appraisal. Neuron Glia Biology 3, 181-189*
- 17 Oberheim, N.A., et al. (2006) *Astrocytic complexity distinguishes the human brain. Trends in Neurosciences 29, 547-553*
- 18 Ransom, B., Behar, T., Nedergaard, M. (2003) *New roles for astrocytes (stars at last). Trends in Neurosciences 26, 520-522*
- 19 Waagepetersen, H.S., et al. (2009) *Energy and amino acid neurotransmitter metabolism in astrocytes. In Astrocytes in (Patho) Physiology of the Nervous System (Parpura, V. and Haydon, P.G., eds), pp. 177-199, Springer*
- 20 Hertz, L. and Zielke, H.R. (2004) *Astrocytic control of glutamatergic activity: astrocytes as stars of the show. Trends in Neurosciences 27, 735- 743*

- 21 Westergaard, N., *et al.* (1996) Evaluation of the importance of transamination versus deamination in astrocytic metabolism of [U-13C]glutamate. *Glia* 17, 160–168
- 22 Sonnewald, U., *et al.* (1997) Glutamate transport and metabolism in astrocytes. *Glia* 21, 56–63
- 23 Kandel, E.R., *et al.* (2000) *Principles of Neural Science*. McGraw-Hill
- 24 Abbott, N.J., *et al.* (2006) Astrocyte-endothelial interactions at the blood–brain barrier. *Nature Reviews Neuroscience* 7, 41–53
- 25 McKenna, M.C., *et al.* (2012) Energy metabolism in the brain, in *Basic Neurochemistry: Molecular, Cellular and Medical Aspects*. (8 edn) (Siegel, G.J., *et al.*, eds), pp. 223–258, Elsevier-Academic Press
- 26 Walls, A.B., *et al.* (2009) Robust glycogen shunt activity in astrocytes: effects of glutamatergic and adrenergic agents. *Neuroscience* 158, 284–292
- 27 Schousboe, A., *et al.* (2010) Functional importance of the astrocytic glycogen-shunt and glycolysis for maintenance of an intact intra/ extracellular glutamate gradient. *Neurotoxicity Research* 18, 94–99
- 28 Schousboe, A., *et al.* (2011) Neuron-glia interactions in glutamatergic neurotransmission: roles of oxidative and glycolytic adenosine triphosphate as energy source. *Journal of Neuroscience Research* 89, 1926–1934
- 29 Brown, A.M. and Ransom, B.R. (2007) Astrocyte glycogen and brain energy metabolism. *Glia* 55, 1263–1271
- 30 Martinez-Hernandez, A., *et al.* (1977) Glutamine synthetase: glial localization in brain. *Science* 195, 1356–1358
- 31 Pellerin, L. and Magistretti, P.J. (1994) Glutamate uptake into astrocytes stimulates aerobic glycolysis: a mechanism coupling neuronal activity to glucose utilization. *Proceedings of the National Academy of Sciences USA* 91, 10625–10629
- 32 Araque, A., *et al.* (1999) Tripartite synapses: glia, the unacknowledged partner. *Trends in Neurosciences* 22, 208–215
- 33 Kimelberg, H.K. (2007) Supportive or information-processing functions of the mature protoplasmic astrocyte in the mammalian CNS? A critical appraisal. *Neuron Glia Biology* 3, 181–189
- 34 Perea, G., *et al.* (2009) Tripartite synapses: astrocytes process and control synaptic information. *Trends in Neurosciences* 32, 421–431
- 35 Arcuino, G., *et al.* (2002) Intercellular calcium signaling mediated by point-source burst release of ATP. *Proceedings of the National Academy of Sciences USA* 99, 9840 – 9845
- 36 Hassinger, T.D., *et al.* (1996) An extracellular signaling component in propagation of astrocytic calcium waves. *Proceedings of the National Academy of Sciences USA* 93
- 37 Newman, E.A. (2003) New roles for astrocytes: regulation of synaptic transmission. *Trends in Neurosciences* 26, 536–542
- 38 Halassa, M.M., *et al.* (2007) The tripartite synapse: roles for gliotransmission in health and disease. *Trends in Molecular Medicine* 13, 54–63
- 39 Hung, J. and Colicos, M.A. (2008) Astrocytic Ca²⁺ waves guide CNS growth cones to remote regions of neuronal activity. *PLoS ONE* 3, e3692

- 40 Halassa, M.M., *et al.* (2009) Astrocytic Modulation of Sleep Homeostasis and Cognitive Consequences of Sleep Loss. *Neuron* 61, 213-219
- 41 Parpura, V., *et al.* (2012) Glial cells in (patho)physiology. *Journal of Neurochemistry* 121, 4-27
- 42 Santello, M. and Volterra, A. (2009) Synaptic modulation by astrocytes via Ca^{2+} -dependent glutamate release. *Neuroscience* 158, 253-259
- 43 Araque, A., *et al.* (1999) Astrocyte-induced modulation of synaptic transmission. *Canadian Journal of Physiology and Pharmacology* 77, 699-706
- 44 Oliet, S.H. and Piet, R. (2004) Anatomical remodelling of the supraoptic nucleus: changes in synaptic and extrasynaptic transmission. *Journal of Neuroendocrinology* 16, 303-307
- 45 Iino, M., *et al.* (2001) Glia-synapse interaction through Ca^{2+} - permeable AMPA receptors in Bergmann glia. *Science* 292, 926-929
- 46 Ni, Y., *et al.* (2007) Vesicular release of glutamate mediates bidirectional signalling between astrocytes and neurons. *Journal of Neurochemistry* 103, 1273-1284.
- 47 Halassa, M.M., *et al.* (2009) Tripartite synapses: roles for astrocytic purines in the control of synaptic physiology and behavior. *Neuropharmacology* 57, 343-346
- 48 Zhang, Q. and Haydon, P.G. (2005) Roles for gliotransmission in the nervous system. *Journal of Neural Transmission* 112, 121-125
- 49 Parpura, V., *et al.* (2010) Regulated exocytosis in astrocytic signal integration. *Neurochemistry International* 57, 451- 459
- 50 Parpura, V. and Zorec, R. (2010) Gliotransmission: exocytotic release from astrocytes. *Brain Research Reviews* 63, 83-92
- 51 Kreft, M., *et al.* (2004) Properties of Ca^{2+} - dependent exocytosis in cultured astrocytes. *Glia* 46, 437-445
- 52 Volterra, A. and Bezzi, P. (2002) Chapter 13: Release of transmitters from glial cells. In *In The Tripartite Synapse: Glia in Synaptic Transmission* (Volterra, A., *et al.*, eds), pp. 164-184, Oxford University Press
- 53 Hertz L., *et al.* (1999) Astrocytes: glutamate producers for neurons. *Journal of Neuroscience Research* 57, 417- 428
- 54 Wolosker, H., *et al.* (1999) Purification of serine racemase: biosynthesis of the neuromodulator D-serine. *Proceedings of the National Acadademy of Sciences USA* 96, 721-725
- 55 Stevens, E.R., *et al.* (2003) D-serine and serine racemase are present in the vertebrate retina and contribute to the physiological activation of NMDA receptors. *Proceedings of the National Academy of Sciences* 100, 6789-6794
- 56 Panatier, A., *et al.* (2006) Glia-Derived D-Serine Controls NMDA Receptor Activity and Synaptic Memory. *Cell* 125, 775-784
- 57 Fields, R.D. and Burnstock, G. (2006) Purinergic signalling in neuron-glia interactions. *Nature Reviews Neuroscience* 7, 423-436
- 58 Conti, F., *et al.* (1994) Cellular localization and laminar distribution of AMPA glutamate receptor subunits mRNAs and proteins in the rat cerebral cortex. . *Journal of Comparative Neurology* 350, 241-259

- 59 Conti, F., *et al.* (1996) Expression of NR1 and NR2A/B subunits of the NMDA receptor in cortical astrocytes. *Glia* 17, 254-258
- 60 Lalo, U., *et al.* (2011) Age-dependent remodelling of ionotropic signalling in cortical astroglia. *Aging Cell* 10, 392-402
- 61 Minelli A., *et al.* (2007) Cellular and subcellular localization of Na⁺/Ca²⁺ exchanger protein isoforms, NCX1, NCX2, and NCX3 in cerebral cortex and hippocampus of adult rat. *Cell Calcium* 41, 221-234
- 62 Oliveira, J.F., *et al.* (2011) Rodent Cortical Astroglia Express In Situ Functional P2X7 Receptors Sensing Pathologically High ATP Concentrations. *Cerebral Cortex* 21, 806-820
- 63 Hua, X., *et al.* (2004) Ca²⁺-dependent glutamate release involves two classes of endoplasmic reticulum Ca²⁺ stores in astrocytes. *Journal of Neuroscience Research* 76, 86-97
- 64 Takemura, H. and Putney Jr, J.W. (1989) Capacitative calcium entry in parotid acinar cells. *Biochemical Journal* 258, 409-412
- 65 Golovina, V.A. (2005) Visualization of localized store-operated calcium entry in mouse astrocytes. Close proximity to the endoplasmic reticulum. *Journal of Physiology* 564, 737-749
- 66 Lalo, U., *et al.* (2011) Ionotropic receptors in neuronal-astroglial signalling: what is the role of "excitable" molecules in non-excitable cells. *Biochimica et Biophysica Acta* 1813, 992-1002
- 67 Kirischuk, S., *et al.* (1997) Na⁺/Ca²⁺ exchanger modulates kainate-triggered Ca²⁺ signaling in Bergmann glial cells in situ. *Journal of the Federation of the American Societies for Experimental Biology* 11, 566-572
- 68 Rojas, H., *et al.* (2008) The activity of the Na⁺/Ca²⁺ exchanger largely modulates the Ca²⁺ signal induced by hypo-osmotic stress in rat cerebellar astrocytes. The effect of osmolarity on exchange activity. *Journal of Physiological Sciences* 58, 277-279.
- 69 Reyes, R.C. and Parpura, V. (2008) Mitochondria modulate Ca²⁺-dependent glutamate release from rat cortical astrocytes. *Journal of Neuroscience* 28, 9682-9691
- 70 Reyes, R.C., *et al.* (2011) Immunophilin deficiency augments Ca²⁺-dependent glutamate release from mouse cortical astrocytes. *Cell Calcium* 49, 23-34
- 71 Montana, V., *et al.* (2006) Vesicular transmitter release from astrocytes. *Glia* 54, 700-715
- 72 Paco, S., *et al.* (2009) Regulation of exocytotic protein expression and Ca²⁺-dependent peptide secretion in astrocytes. *Journal of Neurochemistry* 110, 143-156
- 73 Volterra, A. and Meldolesi, J. (2005) Astrocytes, from brain glue to communication elements: the revolution continues. *Nature Reviews of Neuroscience* 6, 626-640
- 74 Seifert, G., *et al.* (2006) Astrocyte dysfunction in neurological disorders: a molecular perspective. *Nature Reviews of Neuroscience* 7, 194-206
- 75 Gosselin, R.D., *et al.* (2009) Region specific decrease in glial fibrillary acidic protein immunoreactivity in the brain of a rat model of depression. *Neuroscience* 159, 915-925
- 76 Banasr, M. and Duman, R.S. (2008) Glial Loss in the Prefrontal Cortex Is Sufficient to Induce Depressive-like Behaviors. *Biological Psychiatry* 64, 863-870

- 77 Banasr, M., *et al.* (2010) Glial pathology in an animal model of depression: reversal of stress-induced cellular, metabolic and behavioral deficits by the glutamate-modulating drug riluzole. *Molecular Psychiatry* 15, 501-511
- 78 Eng, L.F., *et al.* (2000) Glial fibrillary acidic protein: GFAP-thirty-one years (1969–2000). *Neurochemical Research* 25, 1439-1451
- 79 Cohen-Gadol, A.A., *et al.* (2004) Mesial temporal lobe epilepsy: a proton magnetic resonance spectroscopy study and a histopathological analysis. *Journal of Neurosurgery* 101, 613-620
- 80 Tian, G.F., *et al.* (2005) An astrocytic basis of epilepsy *Nature Medicine* 11, 973–981
- 81 Webster, M.J., *et al.* (2005) Glial fibrillary acidic protein mRNA levels in the cingulate cortex of individuals with depression, bipolar disorder and schizophrenia. *Neuroscience* 133, 453-461
- 82 Rajkowska, G., *et al.* (2002) Layer-specific reductions in GFAP-reactive astroglia in the dorsolateral prefrontal cortex in schizophrenia. *Schizophrenia Research* 57, 127-138
- 83 Johnston-Wilson, N.L., *et al.* (2000) Disease-specific alterations in frontal cortex brain proteins in schizophrenia, bipolar disorder, and major depressive disorder. *Molecular Psychiatry* 5, 142–149
- 84 Sastre, M., *et al.* (2003) Nonsteroidal anti-inflammatory drugs and peroxisome proliferator-activated receptor-gamma agonists modulate immunostimulated processing of amyloid precursor protein through regulation of beta-secretase. *Journal of Neuroscience* 23, 9796–9804
- 85 Sastre, M., *et al.* (2006) Nonsteroidal anti-inflammatory drugs repress β -secretase gene promoter activity by the activation of PPAR γ . *Proceedings of the National Academy of Sciences of the USA* 103, 443-448
- 86 Lee, H.-J., *et al.* (2010) Direct Transfer of α -Synuclein from Neuron to Astroglia Causes Inflammatory Responses in Synucleinopathies. *The Journal of Biological Chemistry* 285, 9262–9272
- 87 Cornell-Bell, A., *et al.* (1990) Glutamate induces calcium waves in cultured astrocytes: long-range glial signaling. *Science* 247, 470-473
- 88 Verkhratsky, A. and Kettenmann, H. (1996) Calcium signalling in glial cells. *Trends in Neurosciences* 19, 346-352
- 89 Khurgel, M., *et al.* (1996) Selective ablation of astrocytes by intracerebral injections of α -aminoadipate. *Glia* 16, 351-358
- 90 Florian, C., *et al.* (2011) Astrocyte-Derived Adenosine and A1 Receptor Activity Contribute to Sleep Loss-Induced Deficits in Hippocampal Synaptic Plasticity and Memory in Mice. *The Journal of neuroscience* 31, 6956-6962
- 91 Dalley, J.W., *et al.* (2004) Prefrontal executive and cognitive functions in rodents: neural and neurochemical substrates. *Neuroscience and biobehavioral reviews* 28, 771-784
- 92 Clark, L. (2004) The neuropsychology of ventral prefrontal cortex: Decision-making and reversal learning. *Brain and Cognition* 55, 41-53
- 93 Goldman-Rakic, P.S. (1995) Architecture of the Prefrontal Cortex and the Central Executive. *Annals of the New York Academy of Sciences* 769, 71-84

- 94 Hernández-González, M., *et al.* (2012) Prefrontal electroencephalographic activity during the working memory processes involved in a sexually motivated task in male rats. *Experimental Brain Research*, 1-11
- 95 Uylings, H.B.M. and van Eden, C.G. (1991) Chapter 3 Qualitative and quantitative comparison of the prefrontal cortex in rat and in primates, including humans. In *Progress in Brain Research* (H.B.M. Uylings, C.G.V.E.J.P.C.D.B.M.A.C. and Feenstra, M.G.P., eds), pp. 31-62, Elsevier
- 96 Uylings, H.B.M., *et al.* (2003) Do rats have a prefrontal cortex? *Behavioural Brain Research* 146, 3-17
- 97 Vertes, R.P. (2006) Interactions among the medial prefrontal cortex, hippocampus and midline thalamus in emotional and cognitive processing in the rat. *Neuroscience* 142, 1-20
- 98 Birrell, J.M. and Brown, V.J. (2000) Medial frontal cortex mediates perceptual attentional set shifting in the rat. *The Journal of neuroscience* 20, 4320-4324
- 99 Kesner, R.P. (2000) Subregional analysis of mnemonic functions of the pre-frontal cortex in the rat. *Psychobiology* 28, 219 -228.
- 100 Ragozzino, M.E., *et al.* (1999) Involvement of the Prelimbic-Infralimbic Areas of the Rodent Prefrontal Cortex in Behavioral Flexibility for Place and Response Learning. *The Journal of neuroscience* 19, 4585-4594
- 101 Rich, E.L. and Shapiro, M.L. (2007) Prelimbic/Infralimbic Inactivation Impairs Memory for Multiple Task Switches, But Not Flexible Selection of Familiar Tasks. *The Journal of neuroscience* 27, 4747-4755
- 102 Martinet, L., *et al.* (2011) Spatial Learning and Action Planning in a Prefrontal Cortical Network Model. *PLoS Computational Biology* 7, 1-21
- 103 Tierney, P.L., *et al.* (2004) Influence of the hippocampus on interneurons of the rat prefrontal cortex. *European Journal of Neuroscience* 20, 514-524
- 104 Paxinos, G. and Watson, C. (2007) *The Rat Brain in Stereotaxic Coordinates (6th ed.)*. Elsevier Academic Press
- 105 Alves, H.N.C., *et al.* (2010) Anesthesia with Intraperitoneal Propofol, Medetomidine, and Fentanyl in Rats. *Journal of the American Association for Laboratory Animal Science* 49, 454-459
- 106 Pascual, O. (2005) Astrocytic Purinergic Signaling Coordinates Synaptic Networks. *Science* 310, 113-116
- 107 Zhang, Q., *et al.* (2004) Fusion-related Release of Glutamate from Astrocytes. *The journal of Biological Chemistry* 279, 12724-12733
- 108 Wood, E.R., *et al.* (1999) The global record of memory in hippocampal neuronal activity. *Nature* 397, 613-616
- 109 Morris, R. (1984) Developments of a water-maze procedure for studying spatial learning in the rat. *Journal of Neuroscience Methods* 11, 47-60
- 110 de Bruin, J.P.C., *et al.* (1994) A behavioural analysis of rats with damage to the medial prefrontal cortex using the morris water maze: evidence for behavioural flexibility, but not for impaired spatial navigation. *Brain Research* 652, 323-333

- 111 Handley, S.L.M., S. (1984) Effects of alpha-adrenoceptor agonists and antagonists in a maze-exploration model of "fear"- motivated behaviour. *Naunyn Schmiedebergs Arch. Pharmacol.* 327, 1-5
- 112 Montgomery, K.C. (1955) The relation between fear induced by novel stimulation and exploratory behaviour. *Journal of Comparative & Physiological Psychology* 48, 254-260
- 113 Lister, R. (1987) The use of a plus-maze to measure anxiety in the mouse. *Psychopharmacology* 92, 180-185
- 114 Hall, C. (1934) Drive and emotionality: factors associated with adjustment in the rat. *Journal of Comparative Psychology*, 89-108
- 115 Hall, C. and Ballachey, E.L. (1932) A study of the rat's behavior in a field: a contribution to method in comparative psychology. *University of California Publications in Psychology*, 1-12
- 116 Simon, P., et al. (1994) Thigmotaxis as an index of anxiety in mice. Influence of dopaminergic transmissions. *Behavioural Brain Research* 61, 59-64
- 117 Sarnyai, Z., et al. (2000) Impaired hippocampal-dependent learning and functional abnormalities in the hippocampus in mice lacking serotonin1A receptors. *Proceedings of the National Academy of Sciences* 97, 14731-14736
- 118 Bundel, D.D., et al. (2011) Loss of System xc-Does Not Induce Oxidative Stress But Decreases Extracellular Glutamate in Hippocampus and Influences Spatial Working Memory and Limbic Seizure Susceptibility. *Journal of Neuroscience* 31, 5792-5803
- 119 Cerqueira, J.J., et al. (2007) The prefrontal cortex as a key target of the maladaptive response to stress. *The Journal of neuroscience* 27, 2781-2787
- 120 Ge, W.-P., et al. (2012) Local generation of glia is a major astrocyte source in postnatal cortex. *Nature* 484, 376-380
- 121 van Zutphen, L.F., et al. (2001) *Principles of Laboratory Animal Science, Revised Edition.*
- 122 Dalley, J.W., et al. (2004) Prefrontal executive and cognitive functions in rodents: neural and neurochemical substrates. *Neuroscience and Biobehavioral Reviews* 28, 771-784
- 123 Bezzi, P. and Volterra, A. (2001) A neuron-glia signalling network in the active brain. *Current Opinion in Neurobiology* 11, 387-394
- 124 Schell, M.J., et al. (1997) D-Serine as a Neuromodulator: Regional and Developmental Localizations in Rat Brain Glia Resemble NMDA Receptors. *The Journal of neuroscience* 17, 1604-1615
- 125 Mothet, J.-P., et al. (2000) D-Serine is an endogenous ligand for the glycine site of the N-methyl-d-aspartate receptor. *Proceedings of the National Academy of Sciences* 97, 4926-4931
- 126 Yang, Y., et al. (2003) Contribution of astrocytes to hippocampal long-term potentiation through release of d-serine. *Proceedings of the National Academy of Sciences* 100, 15194-15199
- 127 Mothet, J.-P., et al. (2005) Glutamate receptor activation triggers a calcium-dependent and SNARE protein-dependent release of the gliotransmitter D-serine. *Proceedings of the National Academy of Sciences of the United States of America* 102, 5606-5611
- 128 Malenka, R.C. and Bear, M.F. (2004) LTP and LTD: an embarrassment of riches. *Neuron* 44, 5-21